

Manuscript Number: CLAY10646R1

Title: Anti-ulcerant kynurenic acid molecules intercalated Mg/Al-layered double hydroxide and its release study

Article Type: Research Paper

Keywords: layered double hydroxide, kynurenic acid, intercalation, in vitro drug release study, anti- ulcerant properties, simulated gastric fluid

Corresponding Author: Dr. László Janovák, Ph.D.

Corresponding Author's Institution: University of Szeged

First Author: Ágota Deák

Order of Authors: Ágota Deák; Edit Csapó, PhD; Ádám Juhász; Imre Dékány, PhD; László Janovák, Ph.D.

Abstract: Kynurenic acid (KYNA) is a product of the tryptophan metabolism and it possess also anti- ulcerant properties, however, the application of KYNA for the treatment of gastroduodenal ulceration is limited, because the concentration of KYNA is very low in human gastric fluid (0.01  $\mu\text{M}$ ). The intercalation of KYNA molecules into biocompatible Mg-Al layered double hydroxides (LDH) lamellae could solve this problem. For this purpose Mg-Al LDH with  $114.96 \pm 0.48$  m<sup>2</sup>/g BET surface area and +0.641 meq/g specific surface charge was synthesized. The intercalation of the anionic target molecules into positively charged LDH layers was carried out with simply ion- exchange reaction. The structure of the obtained KYNA/ LDH hybrid materials were studied by powdered X-ray diffraction (PXRD) and Attenuated total reflection Fourier transform infrared (ATR-FTIR) spectroscopy verifying that the KYNA molecules prefer creating a paraffin type monolayer arrangement. Due to the intercalation process the (003) reflection peaks of initial LDH ( $2\theta=11.39^\circ$ ,  $d(003)=0.775$  nm) shift to lower angles ( $2\theta=4.11^\circ$ ,  $d=2.146$  nm). That means, that the basal space value ( $d_L$ ) of the KYNA-LDH sample was 1.436 nm. The total amount of the intercalated KYNA molecules into LDH layers was measured by fluorescence spectroscopy method. According to the results the drug- loading capacity was about 120 mg KYNA/ g LDH. This ~12% KYNA content of the hybrid materials was also evidenced by thermogravimetric measurements, because the thermal decomposition of the bio-hybrid materials was examined by thermogravimetry (TG) analysis. Our experimental data confirm that the anti- ulcerant KYNA molecules can be safely loaded and stored into LDH's layers forming a new bio-active hybrid material. In addition we also presented by PXRD and gravimetric measurements that prepared LDH layers were almost completely dissolved (~83 wt.%) in the applied simulated gastric fluid (SGF) media (pH=1.5) under 60 min and the encapsulated KYNA molecules released from the destroyed interlayers. Finally, the measured KYNA drug release profile from the bioactive composite material was also presented in SGF media. According to the results 18% of the loaded KYNA molecules were released during 6 hours.

Response to Reviewers: Point-by-point response to the Reviewers' comments  
The Reviewers' comments are always followed by our response highlighted  
in yellow.

Reviewer #2:

First of all, we would like to thank the Reviewer for his very positive  
evaluation of our manuscript, and for the insightful comments which truly  
improved the quality of the manuscript!

With respect,  
László Janovák

Reviewer #2: The paper could be accepted with minor revision of the  
following aspects:

1) Introduction is too long. Please, reduce it almost 50%.  
The Introduction part was reduced and rewritten, only the most important  
sentences and relevant parts were remained in the text. See shortened  
introduction part, line 46-127.

2) Materials:

Please, include country of provenance of the reagents. The country of  
provenance of the reagents was indicated in all cases (see Chapter 2.1.,  
line 130-144).

3) Methods:

Adsorption experiments. Please, explain why the experiments were finished  
after 1 hour. It was time enough to reach equilibrium? The drug  
degrades at longer times?

During the drug intercalation, the prepared KYNA/LDH suspensions were  
stirred for 1 hour at room temperature (25 °C) in order to reach the  
adsorption equilibrium, then were filtered through a fine filter  
(Millipor, 0.22 µm) then the KYNA concentration was determined from the  
spectrofluorometric calibration curves (see line 170-172 in the text).  
The figure below shows a characteristic intercalation kinetic curve and  
it can be seen, that 1 hour was enough time to reach the equilibrium/  
plateau value. This data/ figure is not presented in the article.

Figure. The specific amount of intercalated KYNA molecules (mg KYNA/ g  
LDH) as a function of adsorption time (KYNA/ LDH weight ratio: 0.5)

Characterization: Please, separate the techniques in subsections.  
The techniques were separated in subsections according to your  
suggestion. See Chapter 2.4.1. - 2.4.5.

TGA were done in air or nitrogen? Please, specify.  
During TG measurements, the samples were heated in synthetic air from 25  
to 1000 °C at a heating rate of 5°C/min (Mettler-Toledo TGA/SDTA 851e  
Instrument) (see line 215).

FTIR were done with tablets or powder KBr?

Attenuated total reflection Fourier transform infrared (ATR-FTIR) spectroscopy measurements were performed by a Biorad FTS-60A FT-IR spectrometer by accumulation of 256 scans at a resolution of 4 cm<sup>-1</sup> between 4000 and 500 cm<sup>-1</sup>. Each sample was previously weighted before spectrum acquisition (about 10 ± 1 mg of powder sample) and placed onto the ATR crystal. All spectral manipulations were performed using Thermo Scientific GRAMS/AI Suite software. (see line 205-210).

Results:

Figures 3, 7 and 8. Please, include standard deviations. The KYNA drug intercalation and release measurements, as well as the gravimetrically measured percentage weight loss of the LDH drug carrier were carried out triplicate, and average values are reported. Error bars refer to the standard deviation (see line 173-174, line 230-231). The calculated standard deviation values were indicated in Figures 3, 7 and 8.

Figure 6. Please, correct Y axis. It should be weight loss (% w/w). Figures 6 was corrected according to your suggestion.

Once these corrections will be done, the manuscript could be accepted.

Reviewer #4:

We would like to thank the valuable discussions on this manuscript. Your comments were very useful. Please find our answers according the questions as follows:

With respect,  
László Janovák

Reviewer #4: Deák et al. have demonstrated utilization of layered double hydroxide for drug delivery. The synthetic methodology of intercalating anti-ulcerant kynurenic acid molecule in LDH is presented with release of drug molecules. There have been several reports on use of layered materials (synthetic and natural) for sustained release of therapeutics. However, this manuscript provides study on the new drug molecules. Although the manuscript shows an approach for synthesis of LDH/drug composites and its release study effectively, I recommend this manuscript after addressing following minor comments before considering this manuscript for publication in Applied Clay Science.

Title:

The title of the manuscript is needed to be modified for better understanding of the research presented. I suggest "Anti-ulcerant kynurenic acid molecules intercalated Mg/Al-layered double hydroxide and its release study"

The title was modified according to your suggestion (see line 1-2).

Abstract:

Authors should include, briefly, why it is important to form this intercalated compounds and why it is necessary. First one or two sentences of abstract should focus on this. Detailed description (a paragraph) should also be included in the introduction section.

The abstract section was completed with the followings:

Kynurenic acid (KYNA) is a product of the tryptophan metabolism and it possess also anti- ulcerant properties, however, the application of KYNA for the treatment of gastroduodenal ulceration is limited, because the concentration of KYNA is very low in human gastric juice (0.01  $\mu\text{M}$ ). The intercalation of KYNA molecules into biocompatible LDH lamellae could solve this problem (see line 15-19).

The detailed motivation of this work is also located in Introduction section (see line 84-91 and line 122-127) according to the followings: Some article also reported that the KYNA may prove useful against domoic acid induced gastropathy because it protects against gastroduodenal ulceration (Glavin et al., 1989a). Furthermore, it was also reported that KYNA protects against gastric and duodenal ulceration caused by a poisonous Atlantic shellfish (Glavin and Pinsky, 1989b). However, according to the publication of Turski et. al., the concentration of KYNA increases gradually along the gastrointestinal tract, reaching its highest value at the very end of it and the lowest concentration of KYNA was found in human gastric juice (0.01  $\mu\text{M}$ ) (Turski et al., 2013). Thus, the application of KYNA for the treatment of gastroduodenal ulceration is limited.

In this article the intercalation of neuroprotective and anti- ulcerant KYNA molecules in the biocompatible MgAl-LDH drug carrier system was examined. The quantitative characterization of intercalation and the structural properties of the prepared KYNA pillared LDH composite materials was also reported. In addition, the LDH dissolution and the KYNA drug release profile from the bioactive composite material was also presented in simulated gastric fluid (SGF).

Introduction:

I suggest including a paragraph on other materials, especially inorganic materials – natural clays, silicas – which have been utilized for drug delivery applications and cite related references. e.g. Applied Clay Science 51 (2011) 126-130; Colloid Polym Sci (2009) 287:1071-1076; Journal of biomaterials applications 25 (2), 161-177, 2010.

The Introduction part was completed with the followings:

Layered clay minerals are widely used for their capability to intercalate molecules in the interlayer space. It is also well known that beside the LDH drug carrier, the negatively charged clay minerals such as Montmorillonite [ $(\text{Na,Ca})_{0.33}(\text{Al,Mg})_2(\text{Si}_4\text{O}_{10})(\text{OH})_2 \cdot n\text{H}_2\text{O}$ ] exhibit an excellent sorption property, large specific surface area, cation exchange capacity and drug-carrying capability (Joshi et al., 2009; Patel et al., 2011; Kevadiya et al., 2010). (see line 62-66)

Experimental:

Simulated gastric juice should be replaced with simulated gastric fluid throughout the manuscript.

The "simulated gastric juice (SGJ)" expression was replaced with "simulated gastric fluid (SGF)" throughout the manuscript, in Fig.8. and in Graphical abstract, as well.

Line 177: .....by co-precipitation method. (cite relevant reference)

The Mg/Al-LDH synthesis method was completed with the followings: Mg/Al-LDH was synthesized by co-precipitation method under  $\text{N}_2$  atmosphere to avoid or at least to minimize the contamination by atmospheric  $\text{CO}_2$ , because the adsorption affinity of the carbonate anions derived from atmospheric  $\text{CO}_2$  is very high for LDH. So, in the case of the carbonation of the LDH, the further intercalation and ion- exchange of the  $\text{CO}_3^-$  LDH

would be impossible. (Choy et al., 2004). (See line 147-151 and line 178-179.)

Relevant reference: Choy J.-H., Jung, J.-S., Oh, J.-M., Park, M., Jeong, J., Kang, Y.-K., Han, O.-J. 2004. Layered double hydroxide as an efficient drug reservoir for folate derivatives. *Biomaterials* 25, 3059-3064.

Line 182: is it necessary to have N<sub>2</sub> atmosphere to generate LDH? Line 202; why author need N<sub>2</sub> atmosphere to intercalate drug at room temperature?

See previous answer and line line 147-151, 178-179 in the text .

Line 209: Use "powdered X-ray diffraction (PXRD) profiles instead of "X-ray diffractograms of the powdered"

The "X-ray diffractograms of the powdered" expression was changed to "powdered X-ray diffraction (PXRD)" throughout the manuscript.

Line 269: Fig. 1: Although author mentioned few references for explaining each reflection, it is better to provide PXRD pattern of the standard LDH which author can find from the library in the instrument.

The characterization of the 2:1 Mg/Al-LDH was completed with the followings (see Chapter 3.1. line 254-256):

Fig. 1a illustrate the PXRD pattern of the synthesized Mg/Al-LDH sample and displays the (003) and (006) Bragg reflections characteristic to layered double hydroxides (JCPDS No. 89-0460) (Deng et al., 2015).

The manuscript is well-written with sufficient experiments and characterization. The loading efficiency of drug loading is indeed matching with theoretical capacity and author also studied thoroughly release profiles. It should be accepted for publication after minor revision.



UNIVERSITY OF SZEGED

Faculty of Science and Informatics

Department of Physical Chemistry  
and Materials Sciences

H-6720 Hungary Szeged, Aradi vértanúk tere 1.

Tel: +36-62-544-209 / Fax: +36-62-544-042

---

Dr. Vanessa Prévot

Editors-in-Chief, Applied Clay Science

Université Blaise Pascal, Aubière cedex, France

19 January, 2018

Dear Dr. Vanessa Prévot,

According to some comments received from Editor and Reviewers we have revised our manuscript *Ref. No.: CLAY10646, Anti-ulcerant kynurenic acid molecules intercalated Mg/Al-layered double hydroxide and its release study* (previous title: *Mg/ Al-layered double hydroxide (LDH) as potential drug carrier system for anti- ulcerant kynurenic acid molecules*)

*Authors: Ágota Deák, Edit Csapó, Ádám Juhász, Imre Dékány, László Janovák*

Attached please find the responses to Editor and Reviewers suggestions and questions.

In the name of all co-authors I would like to thank you for the time and efforts while treating our submission.

Yours sincerely,

László Janovák

corresponding author



## Point-by-point response to the Reviewers' comments

The Reviewers' comments are always followed by our response highlighted in yellow.

### Reviewer #2:

First of all, we would like to thank the Reviewer for his very positive evaluation of our manuscript, and for the insightful comments which truly improved the quality of the manuscript!

With respect,

László Janovák

**Reviewer #2:** The paper could be accepted with minor revision of the following aspects:

1) Introduction is too long. Please, reduce in almost 50%.

The Introduction part was reduced and rewritten, only the most important sentences and relevant parts were remained in the text. See shortened introduction part, line 46-127.

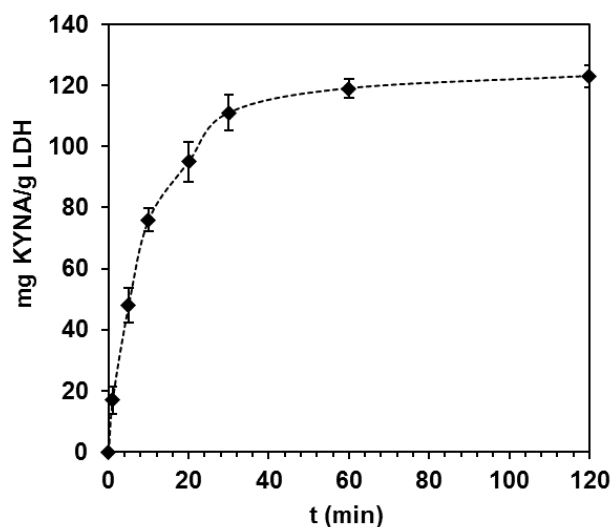
2) Materials:

Please, include country of procedence of the reagents. The country of procedence of the reagents was indicated in all cases (see Chapter 2.1., line 130-144).

3) Methods:

Adsorption experiments. Please, explain why the experiments were finished after 1 hour. It was time enough to reach equilibrium? The drug degradates at longer times?

During the drug intercalation, the prepared KYNA/LDH suspensions were stirred for 1 hour at room temperature (25 ° C) in order to reach the adsorption equilibrium, then were filtered through a fine filter (Millipor, 0.22 μm) than the KYNA concentration was determined from the spectrofluorometric calibration curves (see line 170-172 in the text). The figure below shows a characteristic intercalation kinetic curve and it can be seen, that 1 hour was enough time to reach the equilibrium/ plateau value. This data/ figure is not presented in the article.



1 **Figure.** The specific amount of intercalated KYNA molecules (mg KYNA/ g LDH) as a function of  
2 adsorption time (KYNA/ LDH weigh ratio: 0.5)  
3

4 Characterization: Please, separate the techniques in subsections.

5 The techniques were separated in subsections according to your suggestion. See Chapter 2.4.1. –  
6 2.4.5.

7 TGA were done in air or nitrogen? Please, specify.

8 During TG measurements, the samples were heated in synthetic air from 25 to 1000 °C at a heating  
9 rate of 5°C/min (Mettler-Toledo TGA/SDTA 851e Instrument) (see line 215).  
10

11 FTIR were done with tablets or powder KBr?

12 Attenuated total reflection Fourier transform infrared (ATR-FTIR) spectroscopy measurements were  
13 performed by a Biorad FTS-60A FT-IR spectrometer by accumulation of 256 scans at a resolution of 4  
14  $\text{cm}^{-1}$  between 4000 and 500  $\text{cm}^{-1}$ . Each sample was previously weighted before spectrum acquisition  
15 (about  $10 \pm 1$  mg of powder sample) and placed onto the ATR crystal. All spectral manipulations were  
16 performed using Thermo Scientific GRAMS/AI Suite software. (see line 205-210).  
17

18 Results:  
19

20 Figures 3, 7 and 8. Please, include standard deviations.

21 The KYNA drug intercalation and release measurements, as well as the gravimetrically measured  
22 percentage weight loss of the LDH drug carrier were carried out triplicate, and average values are  
23 reported. Error bars refer to the standard deviation (see line 173-174, line 230-231). The calculated  
24 standard deviation values were indicated in Figures 3, 7 and 8.  
25

26 Figure 6. Please, correct Y axis. It should be weight loss (% w/w).

27 Figures 6 was corrected according to your suggestion.  
28

29  
30 Once these corrections will be done, the manuscript could be accepted.  
31  
32  
33  
34  
35  
36  
37  
38  
39  
40  
41  
42  
43  
44  
45  
46  
47  
48  
49  
50  
51  
52  
53  
54  
55  
56  
57  
58  
59  
60  
61  
62  
63  
64  
65



#### Reviewer #4:

We would like to thank the valuable discussions on this manuscript. Your comments were very useful. Please find our answers according the questions as follows:

With respect,

László Janovák

**Reviewer #4:** Deák et al. have demonstrated utilization of layered double hydroxide for drug delivery. The synthetic methodology of intercalating anti-ulcerant kynurenic acid molecule in LDH is presented with release of drug molecules. There have been several reports on use of layered materials (synthetic and natural) for sustained release of therapeutics. However, this manuscript provides study on the new drug molecules. Although the manuscript shows an approach for synthesis of LDH/drug composites and its release study effectively, I recommend this manuscript after addressing following minor comments before considering this manuscript for publication in Applied Clay Science.

Title:

The title of the manuscript is needed to be modified for better understanding of the research presented. I suggest "Anti-ulcerant kynurenic acid molecules intercalated Mg/Al-layered double hydroxide and its release study"

The title was modified according to your suggestion (see line 1-2).

Abstract:

Authors should include, briefly, why it is important to form this intercalated compounds and why it is necessary. First one or two sentences of abstract should focus on this. Detailed description (a paragraph) should also be included in the introduction section.

The abstract section was completed with the followings:

Kynurenic acid (KYNA) is a product of the tryptophan metabolism and it possess also anti- ulcerant properties, however, the application of KYNA for the treatment of gastroduodenal ulceration is limited, because the concentration of KYNA is very low in human gastric juice (0.01  $\mu\text{M}$ ). The intercalation of KYNA molecules into biocompatible LDH lamellae could solve this problem (see line 15-19).

The detailed motivation of this work is also located in Introduction section (see line 84-91 and line 122-127) according to the followings:

Some article also reported that the KYNA may prove useful against domoic acid induced gastropathy because it protects against gastroduodenal ulceration (Glavin et al., 1989a). Furthermore, it was also reported that KYNA protects against gastric and duodenal ulceration caused by a poisonous Atlantic shellfish (Glavin and Pinsky, 1989b). However, according to the publication of Turski et. al., the concentration of KYNA increases gradually along the gastrointestinal tract, reaching its highest value at the very end of it and the lowest concentration of KYNA was found in human gastric juice (0.01  $\mu\text{M}$ ) (Turski et al., 2013). Thus, the application of KYNA for the treatment of gastroduodenal ulceration is limited.

In this article the intercalation of neuroprotective and anti- ulcerant KYNA molecules in the biocompatible MgAl-LDH drug carrier system was examined. The quantitative characterization of intercalation and the structural properties of the prepared KYNA pillared LDH composite materials was also reported. In addition, the LDH dissolution and the KYNA drug release profile from the bioactive composite material was also presented in simulated gastric fluid (SGF).

Introduction:

I suggest including a paragraph on other materials, especially inorganic materials — natural clays, silicas — which have been utilized for drug delivery applications and cite related references. e.g. Applied Clay Science 51 (2011) 126-130; Colloid Polym Sci (2009) 287:1071-1076; Journal of biomaterials applications 25 (2), 161-177, 2010.

The Introduction part was completed with the followings:

Layered clay minerals are widely used for their capability to intercalate molecules in the interlayer space. It is also well known that beside the LDH drug carrier, the negatively charged clay minerals

1 such as Montmorillonite  $[(\text{Na,Ca})_{0.33}(\text{Al, Mg})_2(\text{Si}_4\text{O}_{10})(\text{OH})_2 \cdot n\text{H}_2\text{O}]$  exhibit an excellent sorption  
2 property, large specific surface area, cation exchange capacity and drug-carrying capability (Joshi et  
3 al., 2009; Patel et al., 2011; Kevadiya et al., 2010). (see line 62-66)

4 Experimental:

5 Simulated gastric juice should be replaced with simulated gastric fluid throughout the manuscript.  
6 The "simulated gastric juice (SGJ)" expression was replaced with "simulated gastric fluid (SGF)"  
7 throughout the manuscript, in Fig.8. and in Graphical abstract, as well.  
8  
9

10 Line 177: .....by co-precipitation method. (cite relevant reference)

11 The Mg/Al-LDH synthesis method was completed with the followings:

12 Mg/Al-LDH was synthesized by co-precipitation method under  $\text{N}_2$  atmosphere to avoid or at least to  
13 minimize the contamination by atmospheric  $\text{CO}_2$ , because the adsorption affinity of the carbonate  
14 anions derived from atmospheric  $\text{CO}_2$  is very high for LDH. So, in the case of the carbonation of the  
15 LDH, the further intercalation and ion- exchange of the  $\text{CO}_3^-$  LDH would be impossible. (Choy et al.,  
16 2004). (See line 147-151 and line 178-179.)

17 Relevant reference: Choy J.-H., Jung, J.-S., Oh, J.-M., Park, M., Jeong, J., Kang, Y.-K., Han, O.-J.  
18 2004. Layered double hydroxide as an efficient drug reservoir for folate derivatives. *Biomaterials* 25,  
19 3059-3064.  
20  
21

22 Line 182: is it necessary to have  $\text{N}_2$  atmosphere to generate LDH? Line 202; why author need  $\text{N}_2$   
23 atmosphere to intercalate drug at room temperature?

24 See previous answer and line line 147-151, 178-179 in the text .  
25

26 Line 209: Use "powdered X-ray diffraction (PXRD) profiles instead of "X-ray diffractograms of the  
27 powdered"

28 The "X-ray diffractograms of the powdered" expression was changed to "powdered X-ray diffraction  
29 (PXRD)" throughout the manuscript.  
30

31 Line 269: Fig. 1: Although author mentioned few references for explaining each reflection, it is better to  
32 provide PXRD pattern of the standard LDH which author can find from the library in the instrument.

33 The characterization of the 2:1 Mg/Al-LDH was completed with the followings (see Chapter 3.1. line  
34 254-256):

35 Fig. 1a illustrate the PXRD pattern of the synthesized Mg/Al-LDH sample and displays the (003) and  
36 (006) Bragg reflections characteristic to layered double hydroxides (JCPDS No. 89-0460) (Deng et al.,  
37 2015).  
38

39 The manuscript is well-written with sufficient experiments and characterization. The loading efficiency  
40 of drug loading is indeed matching with theoretical capacity and author also studied thoroughly release  
41 profiles. It should be accepted for publication after minor revision.  
42  
43  
44  
45  
46  
47  
48  
49  
50  
51  
52  
53  
54  
55  
56  
57  
58  
59  
60  
61  
62  
63  
64  
65

1 **Anti-ulcerant kynurenic acid molecules intercalated Mg/Al-layered double hydroxide**  
2 **and its release study**

3  
4 Ágota Deák<sup>a</sup>, Edit Csapó<sup>a,b</sup>, Ádám Juhász<sup>a,b</sup>, Imre Dékány<sup>a,b</sup>, László Janovák<sup>a,\*</sup>

5 <sup>a</sup>*Department of Physical Chemistry and Materials Science, University of Szeged, H-6720,*  
6 *Szeged, Rerrich B. tér 1, Hungary*

7 <sup>b</sup>*MTA-SZTE Biomimetic Systems Research Group, University of Szeged, H-6720, Szeged,*  
8 *Dóm tér 8, Hungary*

9  
10 \* Corresponding authors. Tel.: +36 62 544 210; Fax: +36 62 544 042.

11 *E-mail address: [janovakl@chem.u-szeged.hu](mailto:janovakl@chem.u-szeged.hu) (L. Janovák)*

12  
13  
14 **Abstract**

15 Kynurenic acid (KYNA) is a product of the tryptophan metabolism and it possess also anti-  
16 ulcerant properties, however, the application of KYNA for the treatment of gastroduodenal  
17 ulceration is limited, because the concentration of KYNA is very low in human gastric juice  
18 fluid (0.01  $\mu\text{M}$ ). The intercalation of KYNA molecules into biocompatible Mg–Al layered  
19 double hydroxides (LDH) lamellae could solve this problem. For this purpose Mg–Al LDH  
20 with  $114.96 \pm 0.48 \text{ m}^2/\text{g}$  BET surface area and  $+0.641 \text{ meq/g}$  specific surface charge was  
21 synthesized. The intercalation of the anionic target molecules into positively charged LDH  
22 layers was carried out with simply ion- exchange reaction. The structure of the obtained  
23 KYNA/ LDH hybrid materials were studied by powdered X-ray diffraction (PXRD) and  
24 Attenuated total reflection Fourier transform infrared (ATR-FTIR) spectroscopy verifying that  
25 the KYNA molecules prefer creating a paraffin type monolayer arrangement. Due to the

26 intercalation process the (003) reflection peaks of initial LDH ( $2\Theta= 11.39^\circ$ ,  $d_{(003)}= 0.775$  nm)  
27 shift to lower angles ( $2\Theta= 4.11^\circ$ ,  $d= 2.146$  nm). That means, that the basal space value ( $\Delta d_L$ )  
28 of the KYNA-LDH sample was 1.436 nm. The total amount of the intercalated KYNA  
29 molecules into LDH layers was measured by fluorescence spectroscopy method. According to  
30 the results the drug- loading capacity was about 120 mg KYNA/ g LDH. This ~12% KYNA  
31 content of the hybrid materials was also evidenced by thermogravimetric measurements,  
32 because the thermal decomposition of the bio-hybrid materials was examined by  
33 thermogravimetry (TG) analysis. Our experimental data confirm that the anti- ulcerant KYNA  
34 molecules can be safely loaded and stored into LDH's layers forming a new bio-active hybrid  
35 material. In addition we also presented by PXRD and gravimetric measurements that prepared  
36 LDH layers were almost completely dissolved (~83 wt.%) in the applied ~~simulated gastric~~  
37 ~~juice (SGJ)~~ simulated gastric fluid (SGF) media (pH=1.5) under 60 min and the encapsulated  
38 KYNA molecules released from the destroyed interlayers. Finally, the measured KYNA drug  
39 release profile from the bioactive composite material was also presented in ~~SGJ~~ SGF media.  
40 According to the results 18% of the loaded KYNA molecules were released during 6 hours.

41

42 **Keywords:** layered double hydroxide, kynurenic acid, intercalation, *in vitro* drug release  
43 study, anti- ulcerant properties, simulated gastric juice fluid

44

## 45 1. Introduction

46 LDHs are a class of anionic lamellar compounds made up of positively charged brucite- like  
47 layers (Trifiro and Vaccari, 1996). The chemical composition of the two layers of  
48 hydrotalcite-type minerals can be given by the following general formula:  
49  $[M^{2+}_{1-x}M^{3+}_x(OH)_2]^{b+} \cdot [A_{b/n}]^{n-} \cdot mH_2O$ , where  $M^{2+}$  represents divalent and  $M^{3+}$  represents  
50 trivalent cations, the value of x may vary in the range of 0.2–0.4, and A is the anion among

51 the cationic layers ( $\text{OH}^-$ ,  $\text{Cl}^-$ ,  $\text{NO}_3^-$ ,  $\text{CO}_3^{2-}$ , and  $\text{SO}_4^{2-}$ ) (Constantino and Nocchetti, 2001).  
52 LDHs have been widely exploited to create new materials for applications in catalysis (Patzkó  
53 et al., 2005; Deák et al., 2016), drug delivery and environmental remediation (Bujdosó et al.,  
54 2009; Goh et al., 2008). MgAl-LDHs are most frequently used as a LDH-based drug carrier  
55 and as evidence of its low toxicity, it is widely used as an antacid (Tarnawski et al., 2000) and  
56 the biocompatibility of this layered material was also reported in the literature (Cunha et al.,  
57 2016, Nagy et al., 2013). LDHs particularly prefer multivalent anions within their interlayer  
58 space due to strong electrostatic interaction and therefore LDHs bearing monovalent anions  
59 like nitrate or chloride ions are good precursors for exchange reactions (Choy et al., 2007).  
60 The solubility and surface charge of LDHs as hydroxides is highly pH-dependent (Bish, 1980;  
61 Deák et al., 2015).

62 Layered clay minerals are widely used for their capability to intercalate molecules in the  
63 interlayer space. It is also well known that beside the LDH drug carrier, the negatively  
64 charged clay minerals such as Montmorillonite  $[(\text{Na,Ca})_{0.33}(\text{Al, Mg})_2(\text{Si}_4\text{O}_{10})(\text{OH})_2 \cdot n\text{H}_2\text{O}]$   
65 exhibit an excellent sorption property, large specific surface area, cation exchange capacity  
66 and drug-carrying capability (Joshi et al., 2009; Patel et al., 2011; Kevadiya et al., 2010). It is  
67 worth mentioning that the pioneering works of Choy' group have led to a rapid development  
68 in the research on both varied LDHs/polymers/anions hybrid systems and pharmaceutical  
69 applications of LDHs especially involving the biocompatibility and toxicity of LDHs and  
70 anti-cancer drugs intercalated LDH materials (Choy et al., 2007). Li et al. also developed anti-  
71 inflammatory drug fenbufen-LDH hybrids and showed that these drug-inorganic hybrid  
72 materials can be used as an effective drug delivery system due to their controlled release  
73 capacity (Li et al., 2004). Yang et al. reported the intercalation of vitamins A, E, and C into  
74 LDHs (Yang et al., 2003). Moreover, in addition to the intercalation of pharmaceutical drugs  
75 into layered materials causing no significant denaturation of the drug molecules, it has also

76 been shown to enhance the internalization of the drug into a target cell without any noticeable  
77 side effects (Oh et al., 2009). Thus, LDHs can not only play a role as a biocompatible-  
78 delivery matrix for drugs but also afford a significant increase in the delivery efficiency  
79 (Posati et al., 2012; Oh et al., 2006).

80 Kynurenic acid (KYNA) is a product of the tryptophan metabolism, it has a neuroprotective  
81 and neuroinhibitory properties (Marosi et al., 2010). According to this the interactions  
82 between the different model peptide fragment of human glutamate receptor and KYNA  
83 molecules has relevance in neuroscience (Juhász et al., 2016). Moreover, experimental data  
84 indicate that KYNA may be neuroprotective and it may be of therapeutic value for several  
85 neurological disorders (Varga et al., 2016). Some article also reported that the KYNA may  
86 prove useful against domoic acid induced gastropathy because it protects against  
87 gastroduodenal ulceration (Glavin et al., 1989a). Furthermore, it was also reported that  
88 KYNA protects against gastric and duodenal ulceration caused by a poisonous Atlantic  
89 shellfish (Glavin and Pinsky, 1989b). However, according to the publication of Turski et. al.,  
90 the concentration of KYNA increases gradually along the gastrointestinal tract, reaching its  
91 highest value at the very end of it and the lowest concentration of KYNA was found in human  
92 gastric juice (0.01  $\mu\text{M}$ ) (Turski et al., 2013). Thus, the application of KYNA for the treatment  
93 of gastroduodenal ulceration is limited.

94 Numerous mathematical models (zero-order, first-order, Weibull, Hixone-Crowell,  
95 Korsmeyere-Peppas, etc) have been developed to describe the release properties of the drug  
96 molecules (Costa and Lobo, 2001). There has not been reported mathematical model in the  
97 literature that takes into account all the important effects, in this way we chose three models  
98 that are widely used in literature. The first-order rate model is a typically used model which  
99 describes the adsorption and/or elimination of certain drugs and states that the drug release  
100 rate depends on its concentration.

101  $C_t = C_0 e^{-kt}$  (1)

102 where  $C_0$  is the initial concentration of drug in the drug formulation,  $C_t$  is the concentration of  
103 drug in the drug formulation at time  $t$ , and  $k$  is the first-order release constant with units of  
104 reciprocal time.

105 Presently, many authors utilize the semi-empirical power law model that was proposed by  
106 Korsmeyer and Peppas (Peppas and Merrill, 1977). The model was developed to specifically  
107 model the release of a drug molecule from a polymeric matrix, such as a hydrogel using the  
108 following equation:

109  $C_t = C_0 k_m t^n$  (2)

110 where  $C_0$  is the initial concentration of drug in the drug formulation,  $C_t$  is the concentration of  
111 released drug at time  $t$ ,  $k_m$  is the kinetic constant and  $n$  the release index, indicating the  
112 mechanism of the drug release. At  $n > 0.45$ , non Fickian diffusion is observed, while  $n \leq 0.45$   
113 represents the Fickian diffusion mechanism. The  $n$  values refer to the geometries of the  
114 particles; in the diffusion-controlled release if the value of  $n$  is between 0.45 and 0.43, the  
115 geometries are slab, cylinder or sphere, respectively.

116 Many times the drug release process can be modeled with the classical Fick's diffusion  
117 equation or with the simplified Higuchi expressions (Siepmann and Peppas, 2011). Higuchi  
118 was the first in 1961 who described the release of the drug from an insoluble matrix based on  
119 Fickian diffusion. The Higuchi model is valid for the systems where the initial drug  
120 concentration in the matrix is much higher than the solubility of the drug.

121  $C_t = k_H \sqrt{t}$  (3)

122 where  $C_t$  is the concentration of drug in the drug matrix at time  $t$  and  $k_H$  is the Higuchi  
123 dissolution constant.

124 In this article the intercalation of neuroprotective and anti-ulcerant KYNA molecules in the  
125 biocompatible MgAl-LDH drug carrier system was examined. The quantitative

126 characterization of intercalation and the structural properties of the prepared KYNA pillared  
127 LDH composite materials was also reported. In addition, the LDH dissolution and the KYNA  
128 drug release profile from the bioactive composite material was also presented in ~~simulated~~  
129 ~~gastric juice (SGJ)~~ simulated gastric fluid (SGF).

130

## 131 2. Materials and methods

### 132 2.1. Reagents

133 For the synthesis of layered double hydroxides magnesium nitrate hexahydrate  
134 ( $\text{Mg}(\text{NO}_3)_2 \cdot 6\text{H}_2\text{O}$ , 98%; Sigma-Aldrich, United Kingdom), and aluminum nitrate nonahydrate  
135 ( $\text{Al}(\text{NO}_3)_3 \cdot 9\text{H}_2\text{O}$ , 99.7%; Molar Chemicals Kft., Hungary) were used as precursors.  
136 Kynurenic acid (KYNA) was obtained from Sigma-Aldrich, United Kingdom. The sodium  
137 dodecyl sulfate ( $\text{C}_{12}\text{H}_{25}\text{NaO}_4\text{S}$ , 98%), hydrochloric acid (HCl, 37%) were obtained from  
138 Molar Chemicals Kft., Hungary. The pH was adjusted with sodium hydroxide (NaOH,  
139 99.80%) and hydrochloric acid (HCl, 37%) which were obtained from Molar Chemicals Kft.,  
140 Hungary. The ~~SGJ~~ SGF media was prepared using pepsin (1:10000 NF; 2000 u/g activity)  
141 and hydrochloric acid (HCl, 37%) obtained from Molar Chemicals Kft., Hungary and  
142 potassium chloride (KCl, 99.5-100%) obtained from Reanal, Hungary. Furthermore, sodium  
143 chloride (NaCl, 99.98%), sodium phosphate dibasic dodecahydrate ( $\text{Na}_2\text{HPO}_4 \cdot 12\text{H}_2\text{O}$ ,  
144 100.3%) and sodium dihydrogen phosphate monohydrate ( $\text{NaH}_2\text{PO}_4 \cdot \text{H}_2\text{O}$ , 99%) were  
145 obtained from Molar Chemicals Kft., Hungary and were used for preparing PBS buffer. All  
146 aqueous solutions were made using deionized water.

147

### 148 2.2. Synthesis of 2:1 Mg/Al-LDH

149 Mg/Al-LDH was synthesized by co-precipitation method under  $\text{N}_2$  atmosphere to avoid or at  
150 least to minimize the contamination of LDH by atmospheric  $\text{CO}_2$ , because the adsorption



151 affinity of the carbonate anions derived from atmospheric CO<sub>2</sub> is very high for LDH (Choy et  
152 al., 2004). So, in the case of the carbonation of the LDH, the further intercalation and ion-  
153 exchange of the CO<sub>3</sub><sup>-</sup>- LDH would be impossible. During the synthesis 25.64 g of Mg(NO<sub>3</sub>)<sub>2</sub> ·  
154 6 H<sub>2</sub>O and 18.76 g of Al(NO<sub>3</sub>)<sub>3</sub> · 9H<sub>2</sub>O were dissolved in 300 mL of distilled water under  
155 vigorous stirring and nitrogen atmosphere at room temperature. The molar ratio of Mg:Al was  
156 2:1. Then, 200 mL of 1.875 mol/L concentration of NaOH was added dropwise to the first  
157 solution to obtain the pH=13. The resulting mixture was vigorously stirred at 80°C  
158 temperature under nitrogen atmosphere for 17 hours and aged at 80°C for 3 days. The  
159 resulting precipitate was separated by centrifugation, washed with distilled water twice and  
160 dried in an oven at 60°C overnight.

161

### 162 2.3. Intercalation of KYNA molecules into LDH layers

163 First, the KYNA/LDH weight ratio was systematically changed in order to determine the  
164 maximal intercalation capacity of the LDH layers for the KYNA drug molecules. During this  
165 experiments a calibration series was made from 2 mM KYNA stock solution using double  
166 dilutions and the KYNA concentration was determined by fluorometric measurements. The  
167 fluorescence spectra were recorded by a Horiba Jobin Yvon Fluoromax-4 spectrofluorometer  
168 (excitation at  $\lambda = 350$  nm). The KYNA concentration was quantified by the determined  
169 spectrofluorometric calibration curve between 355-550 nm emission wavelength range and at  
170 a wavelength maximum of  $\lambda_{\max} = 380$  nm. During the adsorption measurements, the KYNA  
171 weight ratio was 0; 0.025; 0.05; 0.1; 0.165; 0.3 0.5 referred to the LDH host lamellae. The  
172 prepared KYNA/LDH suspensions were stirred for 1 hour at room temperature (25 ° C) in  
173 order to reach the adsorption equilibrium, then were filtered through a fine filter (Millipor,  
174 0.22  $\mu\text{m}$ ) than the KYNA concentration was determined from the spectrofluorometric

175 calibration curves. The experiments were carried out triplicate, and average values are  
176 reported. Error bars refer to the standard deviation.

177 In the continuation, the amount of intercalated anionic substance (KYNA) was set at 30 wt%  
178 based on the LDH mass, i.e. the anionic KYNA/LDH weight ratio was 300 mg KYNA / g  
179 LDH. During the intercalation, 30 mg of KYNA was added to 10 ml of 1 wt% LDH  
180 suspension and stirred at 25°C for 48 hours under a nitrogen atmosphere to avoid the  
181 contamination of LDH by atmospheric CO<sub>2</sub>. The pH of the LDH suspensions was adjusted to  
182 10.0 by dropwise addition of 1 mol/L concentration of NaOH solution. The reaction product  
183 was filtered, washed with distilled water to remove adhered KYNA molecules, and dried at 60  
184 °C in an oven for 24 h.

185

## 186 2.4. Methods of sample characterization

### 187 2.4.1. PXRD measurements

188 The X-ray diffractograms of the powdered 2:1 Mg/Al-LDH and the KYNA intercalated LDH  
189 layers were recorded on a Philips X ray diffractometer (PXRD) with CuK<sub>α</sub> (= 0.1542 nm) as  
190 the radiation source at ambient temperature in the 2–40° and 2.5–15° (2 $\Theta$ ) range applying  
191 0.02° (2 $\Theta$ ) step size.

192

### 193 2.4.2. Determination of surface charge of LDH samples

194 The surface charges of the LDH samples were measured in a particle charge detector (PCD-  
195 02 MÜTEK) with manual titration. In the course of a titration process, the surface charges of  
196 the studied samples were compensated by oppositely charged sodium dodecyl sulfate (SDS)  
197 surfactants with concomitant streaming potential measurements. During the titration process,  
198 10 mL of a 0.1% LDH (pH=10) was added to the test cell of the PCD, and was titrated with  
199 oppositely charged surfactant (SDS) solution. The equimolar amount of surfactant was

200 calculated from the surfactant amounts added at the charge compensation point (where  
201 streaming potential = 0 mV) and was normalized to the amount of titrated sample (meq/g).

202

#### 203 **2.4.3. Determination of specific surface area of LDH sample (BET measurement)**

204 The specific surface area of the LDH sample was determined by BET method from N<sub>2</sub>  
205 adsorption isotherms at  $77 \pm 0.5$  K (Micromeritics Gemini 2375 Surface Area Analyzer).  
206 Before the adsorption measurements the samples were evacuated ( $10^{-5}$  mmHg) at 100°C  
207 overnight.

208

#### 209 **2.4.4. ATR-FTIR spectroscopy measurements**

210 **Attenuated total reflection Fourier transform infrared (ATR-FTIR) spectroscopy**  
211 measurements were performed by a Biorad FTS-60A FT-IR spectrometer by accumulation of  
212 256 scans at a resolution of  $4 \text{ cm}^{-1}$  between 4000 and  $500 \text{ cm}^{-1}$ . **Each sample was previously**  
213 **weighted before spectrum acquisition (about  $10 \pm 1$  mg of powder sample) and placed onto**  
214 **the ATR crystal.** All spectral manipulations were performed using Thermo Scientific  
215 GRAMS/AI Suite software.

216

#### 217 **2.4.5. TG measurements**

218 The thermal behavior of the LDH drug carrier, KYNA/LDH composite and KYNA and the  
219 KYNA content of the composite were investigated with thermogravimetric (TG) analysis.  
220 During TG measurements, the samples were heated in **synthetic air** from 25 to 1000°C at a  
221 heating rate of 5°C/min (Mettler-Toledo TGA/SDTA 851<sup>e</sup> Instrument).

222

223 2.5. Dissolution experiment of LDH in acidic ~~SGJ~~ SGF media

224 The dissolution process of the LDH drug carrier was investigated in the presence of the  
225 ~~simulated gastric juice (SGJ)~~ simulated gastric fluid (SGF) at pH= 1.5 which was prepared  
226 with a buffer mixture composed of 0.2 M HCl solution and 0.2 M KCl solution, to which  
227 pepsin was added at a ratio of 10 U/ml (Guérin et al., 2003; Cunha et al., 1997). During the  
228 process 1.491 g of KCl and 0.5 g of pepsin were dissolved in 100 mL of distilled water under  
229 vigorous stirring and 1.67 mL of 37% concentration of HCl was added dropwise to the ~~SGJ~~  
230 SGF solution to obtain the pH at 1.5. Then, 1.0 g of LDH powder sample was added to the  
231 ~~SGJ~~ SGF solution. The concentration of LDH in ~~SGJ~~ SGF solution was 0.01 g/mL. The  
232 dissolution of LDH was followed by gravimetrically measurements and the degradation of  
233 LDH was also recorded with PXRD measurements (using Philips X ray diffractometer with  
234  $\text{CuK}_\alpha$  (= 0.1542 nm) as the radiation source at ambient temperature in the 2–30° (2 $\Theta$ ) range  
235 applying 0.02° (2 $\Theta$ ) step size.). The weight- loss measurements were carried out triplicate,  
236 and average values are reported with the calculated standard deviations.

237

238 2.6. In vitro drug release experiments

239 The in vitro experiments were carried out using a dialysis tubing cellulose membrane (typical  
240 molecular weight cut-off= 12-14 kDa from Sigma Aldrich). Briefly, 1 mL of KYNA solution  
241 (c= 1.6 mg/mL) or KYNA/LDH dispersion in PBS buffer (c= 1.6 mg/mL, KYNA content:  
242 ~12%), (pH=6.70) was pipetted into the tube membrane (d=1 cm, l=10 cm) then immersed  
243 into 100 mL of PBS solution (at pH= 6.70 and 1.50) in a vertical position. The 100 mL of  
244 PBS solution with the carefully closed membrane was stirred continuously with a magnetic  
245 stirrer and the release experiments were carried out at 37.0 °C using a water bath. Samples  
246 were taken every 2.5 minutes in the first 10 minutes, then were taken in the 15<sup>th</sup> and 20<sup>th</sup>  
247 minutes. After 20 minutes the samples were taken in each 10 minutes until the first hour and

248 then were taken after 30 minutes in every hour. Measurements were performed in 240 min.  
249 The presence of kynurenic acid was recorded with a diode array spectrophotometer (Ocean  
250 Optics USB2000; USA) in the  $\lambda = 250\text{--}350$  nm range using a 1 cm quartz cuvette. The  
251 released kynurenic acid concentration was quantified by the previously determined  
252 spectrophotometric calibration curve at a wavelength maximum of  $\lambda_{\text{max}} = 311$  nm. To  
253 determine the value of kinetic constants of the applied release kinetic models, the sum of the  
254 square of differences between the measured and predicted concentration values have been  
255 minimalized using a spreadsheet based computer application for nonlinear parameter  
256 estimation (Juhász et al., 2016).

257

### 258 3. Results and discussion

#### 259 3.1. Characterization of the 2:1 Mg/Al-LDH

260 Fig. 1a illustrates the PXRD pattern of the synthesized Mg/Al-LDH sample and displays the  
261 (003) and (006) Bragg reflections characteristic to layered double hydroxides (JCPDS No. 89-  
262 0460) (Deng et al., 2015). These peaks are positioned at an angle of  $11.39^\circ$  ( $2\Theta$ ) ( $d_{(003)} = 0.77$   
263 nm) and the peak representing the secondary reflection is at an angle of  $22.82^\circ$  ( $2\Theta$ ) ( $d_{(006)} =$   
264 0.39 nm). In addition, further characteristic reflection was observed at angle of  $34.39^\circ$  ( $2\Theta$ )  
265 ( $d_{(009)} = 0.26$  nm) which is the (009) reflection characteristic to the sample (Costa et al.,  
266 2008). The surface charge value of LDH was determined by charge titration (Szabó et al.,  
267 2013). The streaming potentials of diluted, 0.1 wt.% LDH suspension (pH=10) was measured  
268 in a Műtek PCD02 apparatus, while adding oppositely charged NaDS surfactant solution to  
269 the system. A typical charge titration curve is presented in Fig. 1b. The measured initial  
270 streaming potential of layered LDH was positive (+704 mV). This value gradually decreased  
271 upon addition of the oppositely charged 0.1% anionic SDS solution, and reached 0 mV after  
272 the addition of 1.8 ml of surfactant solution. At this point (i.e., the charge equivalence point or

273 c.e.p.), the negatively charged anionic surfactant molecules compensated the positive charge  
274 of LDH in the aqueous suspension. Due to the surface adsorption of the SDS molecules on the  
275 hydrophilic LDH lamellae, the obtained hydrophobized sample was sedimented from the  
276 aqueous media after the titration process (see inserted photos). Based on the charge titration  
277 data, the specified charge of LDH at pH= 10 was +0.641 meq/g LDH. The positive surface  
278 charge of conventional LDH layers of lamellar structure is well-known in the literature  
279 (Glavin et al., 1989a), and creates the basis of its widespread utilization for the adsorption of  
280 various negatively charged molecules (Choy et al., 2007; Fudala et al., 1999).

281 The BET adsorption isotherm of the LDH sample reveals type II isotherm, expressing  
282 multilayer N<sub>2</sub> adsorption, without significant hysteresis loops between the adsorption and  
283 desorption branches (Fig. 2a). The analysis of the N<sub>2</sub> adsorption isotherm by the t-plot method  
284 (Fig. 2b, inset) shows that the sample has a nonporous structure. The BET- method was used  
285 to calculate the surface area of the LDH which was  $114.96 \pm 0.48 \text{ m}^2/\text{g}$ .

286

### 287 3.2. Characterization of the intercalated kynurenic acid in LDH drug carrier

288 The prepared positively charged (+0.641 meq/g) LDH lamellae with relatively high specific  
289 surface area ( $114.96 \pm 0.48 \text{ m}^2/\text{g}$ ) was suitable for the intercalation of negatively charged  
290 guest molecules. The intercalation capacity of the KYNA drug molecules into LDH layers  
291 was measured by fluorescence spectroscopy method (Fig. 3). During the experiments, the  
292 KYNA content of the samples was systematically changed from 2.5 to 50 wt.%. The obtained  
293 results presented in Fig. 3 showed that with the increasing weight ratio of KYNA/LDH the  
294 amount of intercalated KYNA is also increasing and the determined drug- loading capacity  
295 was about 120 mg KYNA/ g LDH. Considering that the measured surface charge of LDH was  
296 +0.641 meq/g LDH and the molecular weight of KYNA (189.16 g/mol), the calculated

297 theoretical intercalated amount of KYNA was 121 mg KYNA/ g LDH. This result is in good  
298 agreement with the experimentally determined value (~12%).

299

### 300 3.2.1. **PXRD** analysis of KYNA intercalation

301 Fig. 4 illustrates the **PXRD** patterns for the Mg/Al-LDH intercalated with KYNA compared  
302 with the initial LDH material. The intercalation of KYNA in LDH has significant influence on  
303 the **PXRD** pattern of LDH at pH=10. The well-crystallized LDH structure with a (003)  
304 diffraction peak positioned at an angle of  $11.39^\circ$  ( $2\theta$ ) shows another (003) diffraction peak  
305 centered at 2.146 nm at a lower  $2\theta$  angle ( $4.11^\circ$ ). The interlayer spacing increases by 1.371  
306 nm in comparison with initial positively charged LDH layers, which shows an interlayer  
307 spacing of 0.775 nm indicating the successful intercalation of drug anions between the  
308 interlayer regions.

309 As Cavani et al. (1991) mentioned, the thickness of the brucite-like layer of LDH is 0.48 nm,  
310 the gallery height in the KYNA-pillared material is 1.666 nm. A gallery height of 1.666 nm  
311 suggests a paraffin type monolayer arrangement (Betega de Paiva et al., 2008; Chiu et al.,  
312 2014) of the intercalated KYNA, with their main axis perpendicular to the layer and the anion  
313 carboxyl groups interacting with positively charged layer surfaces. The suspected structure,  
314 i.e. the paraffin type monolayer arrangement of the obtained LDH/ KYNA composite is also  
315 presented in Fig. 4.

316

### 317 3.2.2. *FT-IR spectra*

318 The FT-IR spectra of the KYNA intercalated in Mg/Al-LDH are presented in Fig. 5. The FT-  
319 IR spectra of initial LDH and pure KYNA are also illustrated for comparison. Fig. 5a shows  
320 the spectrum of nitrate-LDH, a broad absorption band at  $3450\text{ cm}^{-1}$  which is due to the  
321 stretching vibration of the hydroxyl groups of the LDH layers and water molecules from the

322 interlayer space. The band at  $1383\text{ cm}^{-1}$  was assigned to stretching vibration of  $\text{NO}_3^-$  (Aisawa  
323 et al., 2015). This strong absorption peak of the  $\text{NO}_3^-$  was decreased after the ion-exchanged  
324 reaction, supporting that  $\text{NO}_3^-$  was replaced by the KYNA molecule (Fig. 5b).  
325 In the spectrum of KYNA (Fig. 5c) the band at  $3474\text{ cm}^{-1}$  was derived from the stretching  
326 vibrations of  $-\text{O}-\text{H}$  bonds in the carboxyl group. The band centered at  $3431\text{ cm}^{-1}$  is due to  
327 OH bonded to the quinoline ring and the signal seen at  $3076\text{ cm}^{-1}$  is attributed to the C-H  
328 bonds of the quinoline ring. Furthermore, the band at  $2968\text{ cm}^{-1}$  corresponds to stretch  
329 vibrations of the C-H bonds of benzyl and quinoline rings and the signal at  $2718\text{ cm}^{-1}$   
330 corresponds to the double bond  $\text{N}=\text{C}$  in the quinoline ring (López et al., 2014). The  
331 asymmetric and symmetric COO stretching is obtained between  $1700\text{-}1400\text{ cm}^{-1}$ , those at  
332  $1631, 1595, 1415$  and  $1247\text{ cm}^{-1}$  were attributed to  $\nu(\text{C}=\text{O})$ ,  $\nu_{\text{as}}(\text{COO})$ ,  $\nu_{\text{s}}(\text{COO})$  and  $\nu(\text{C}-\text{N})$ ,  
333 respectively. (Geng et al., 2009; Ibrahim et al., 2005). After intercalation, the characteristic  
334 bands of KYNA were observed at  $1631, 1595, 1415, 1247\text{ cm}^{-1}$  in the case of KYNA/LDH  
335 (Fig. 5b). So, according to the evaluation of the IR spectra, the intercalation of KYNA  
336 molecules into the LDH lamellae was also proved.

337

### 338 3.2.3. Thermal analysis

339 Thermogravimetric analysis of the initial LDH clay and the synthesized composites provides  
340 useful information regarding the thermal stability and thermal decomposition temperature of  
341 the materials. The TG curve of powdered KYNA/ LDH pillared composite is illustrated in  
342 Fig. 6. The corresponding TG curves for pure KYNA and initial Mg/Al-LDH are also  
343 presented for comparison.

344 In the LDH, the thermal decomposition stages are generally overlapped and the exact  
345 temperature range of each stage depends largely on LDH type, heating rate and atmosphere  
346 ( $\text{N}_2$  or  $\text{O}_2$ ) (Benício et al., 2015). According to the literature data, LDH thermal behavior is



347 usually characterized by two main transition stages: (i) an endothermic process from room  
348 temperature to about 200 °C that corresponds to adsorbed and interlamellar water loss; this  
349 stage is reversible and occurs without lamellar structure collapse; and (ii) the second stage  
350 occurs with temperatures ranging from 200 to about 6-800 °C, and corresponds to lamellar  
351 hydroxyl group loss (dehydroxylation) as well as anions loss (Benício et al., 2015). In the case  
352 of our LDH sample, both weight losses can be observed. The interlamellar water content was  
353 15.7 wt.% (first step up until ~245 °C), while after about 650 °C, the remaining weight was  
354 53.7 wt.%. It can be also seen, that the heat degradation of the pure KYNA was occurred  
355 between 150 and 650 °C and after about this temperature, the mass loss of organic KYNA  
356 was complete (dashes line). Compared the corresponding TG curves, it can be determined that  
357 the remaining weigh difference between the KYNA/ LDH composite and the LDH sample  
358 was 13.9 wt.%. Fig. 3 shows that the maximum adsorption capacity of the LDH clay lamellae  
359 was about 120 mg KYNA/ g LDH. The thermogravimetric results were confirmed this ~12  
360 wt.% KYNA content of the KYNA pillared composite material.

361

### 362 3.3. Dissolution properties of LDH clay in **SGJ SGF** media

363 The dissolution properties of the LDH drug carrier in acidic pH was investigated  
364 gravimetrically and the acidic dissolution, i.e. the destruction of lamellae was also followed  
365 up by **PXRD** measurements (Fig. 7) The dissolution profile of LDH at pH= 1.5 was exhibited  
366 a very fast process: after about 30 minutes, more than 70 wt.% of the initial LDH weight was  
367 disappeared and at the end of the experiment, near 83% of LDH were completely dissolved in  
368 the applied **SGJ SGF** media after 360 minutes (Fig. 7a). The corresponding **PXRD** patterns of  
369 the LDH is presented in Fig. 7b and gives information about the LDH structure during the  
370 dissolution experiment. It can be observed that the intensity of the characteristic peaks of the  
371 well-crystallized LDH was continuously decreased, i.e. the (003) diffraction peak positioned

372 at an angle of  $11.39^\circ$  ( $2\Theta$ ) was shown decreasing intensity. This phenomenon is obviously  
373 due to dissolution of LDH drug carrier at pH= 1.5.

374

#### 375 3.4. *In vitro* drug release properties of the samples

376 The release properties of KYNA were studied at the pH of human saliva (Baliga et al., 2013;  
377 Pietrzyńska and Voelkel, 2017) at a value of 6.70 and at pH of **SGJ SGF** (pH=1.50), as well.

378 The release study of the KYNA/LDH have also been performed at pH=1.5. Fig. 8 presents the  
379 drug release profiles which were carried out over a period of 240 min and at body temperature  
380 ( $37^\circ\text{C}$ ) and in physiological saline. The released concentration of drug were determined  
381 spectrophotometrically. The solubility and thus the release rate of anionic KYNA depends on  
382 pH (Varga et al., 2016). Thus, on Fig. 8a, a significant difference can be seen on the release  
383 rate of KYNA between pH= 6.70 and 1.50 under the same experimental condition. Due to the  
384 higher solubility of the KYNA molecules at pH= 6.70, the percentage amount of the released  
385 drug molecules were continuously increased up to 180 min and after three hours it was  
386 reached the 90% plateau value. However, at low pH (=1.50), the release of the KYNA was  
387 obviously slower process and the measured maximum value was only about 40%, because in  
388 this pH the KYNA molecules were formed heterogeneous precipitate instead of a clear  
389 homogenous solution (pH=6.70) (see inserted photos). In the case of KYNA release from  
390 concentrated solutions via the fitted (Fig. 8b) first-order rate model (Eq. 1) the following rate  
391 constant values ( $k$ ) were provided:  $4.74 \cdot 10^{-5} \text{ s}^{-1}$  and  $5.91 \cdot 10^{-5} \text{ s}^{-1}$  at pH=6.70 and pH=1.50,  
392 respectively. As regarding the composite sample, drug release profile for KYNA/LDH at pH=  
393 1.5 was exhibited a delayed drug release rate compared to the pure KYNA at the same pH.  
394 This is because the kinetic of the release process is controlled by the LDH, so the diffusion  
395 rate is significantly decreased. The determined  $k$  value was  $1.49 \cdot 10^{-5} \text{ s}^{-1}$  in this case. The  
396 corresponding half-life values ( $t_{1/2} = 4.1$  and  $3.3$  h for KYNA at pH=6.70 and 1.50,

397 respectively) are smaller than the half-life value of composite sample ( $t_{1/2} = 12.9$  h) at  
398 pH=1.50. The kinetic constant, release index and correlation coefficients ( $R^2$ ) values, which  
399 are summarised in Table 1 indicate what processes are controlled by the suggested release  
400 mechanism. Based on the values of correlation coefficients release of the KYNA from the  
401 KYNA/LDH composite was well described by the first-order rate model, while the drug  
402 release from concentrated solutions agreed with the Korsmeyer–Peppas model. The observed  
403 low release index values ( $n = 0.43$  and  $0.38$  for KYNA at pH=6.70 and 1.50, respectively)  
404 suggest the existing of Fickian diffusion mechanism which absolutely corresponds to the  
405 experimentally arranged conditions. Moreover, this model clearly shows the appearance of  
406 non Fickian diffusion ( $n = 0.46$  for KYNA/LDH at pH = 1.50) in the case of the composite  
407 where combination of drug diffusion and carrier erosion result the anomalous process.

408 This result allows to conclude that the rate determining step for release of KYNA from the  
409 KYNA/LDH composite may be depending on the following conditions: (i) dissolution of  
410 LDH lamellae; (ii) ion-exchange reaction between KYNA and LDH and (iii) release of  
411 KYNA from LDH host lamellae. These data indicate that the Mg/Al-LDH could be an  
412 adequate drug carrier system for the neuroprotective and anti- ulcerant KYNA molecules at  
413 low pH.

414

#### 415 **4. Conclusions**

416 This study demonstrated the intercalation of anti- ulcerant KYNA molecules into a layered  
417 inorganic host, LDH, which was carried out with a simply ion- exchange reaction. The **PXRD**  
418 studies showed a paraffin type monolayer arrangement for anti-ulcerant drug molecules into  
419 the synthesized KYNA/ LDH hybrid material. The drug loading capacity of the 2:1 Mg/Al-  
420 LDH was studied by fluorescence spectroscopy method and the obtained ~12% KYNA  
421 content was in good agreement with the theoretical value calculated from the +0.641 meq/g

422 surface charge of the LDH lamellae. Moreover, this ~12% KYNA content of the hybrid  
423 materials was also confirmed by thermogravimetric (TG) measurements.  
424 Next, it was also demonstrated by gravimetric and PXRD measurements, that the prepared  
425 LDH was almost completely dissolved (~83 wt.%) in the applied simulated gastric juice  
426 (SGJ) fluid (SGF) media at pH=1.5. The *in vitro* release studies showed that due to the higher  
427 solubility of the KYNA molecules at pH= 6.70 a significant difference can be seen on the  
428 release rate of KYNA between pH= 6.70 ( $t_{1/2} = 4.1$  h) and 1.50 ( $t_{1/2} = 3.3$  h) under the same  
429 experimental condition. The drug release from KYNA/ LDH composite material at pH= 1.5  
430 was observed a delayed drug release profile ( $1.49 \cdot 10^{-5} \text{ s}^{-1}$ ) compared to the pure KYNA ( $t_{1/2}$   
431 = 12.9 h) at the same pH. The obtained results gives a proof to us that the chosen LDH host  
432 molecule could be an adequate drug carrier system for the neuroprotective and anti- ulcerant  
433 KYNA molecules at gastric pH, used for peptic ulcer diseases.

434

#### 435 **Acknowledgements**

436 The authors are very thankful for the financial support from the Hungarian Scientific  
437 Research Fund (OTKA) K 116323 and the project named GINOP-2.3.2-15-2016-00034. This  
438 paper was supported by the János Bolyai Research Scholarship of the Hungarian Academy of  
439 Sciences (E. Csapó). This paper was supported by the UNKP-17-4 New National Excellence  
440 Program of the Ministry of Human Capacities (L. Janovák).

441

#### 442 **References**

443 Aisawa, S., Ohnuma, Y., Hirose, K., Takahashi, S., Hirahara, H., Narita, E., 2015.  
444 Intercalation of nucleotides into layered double hydroxides by ion-exchange reaction. Applied  
445 Clay Science. 28, 137– 145.

446 Baliga, S., Muglikar, S., Kale, R., 2013. Salivary pH: A diagnostic biomarker. *J. Indian Soc.*  
447 *Periodontol.* 17 (4), 461–465.

448 Benício, L. P. F., Silva, R. A., Lopes, J. A., Eulálio, D., Menezes dos Santos, R. M., Angelo  
449 de Aquino, L., Vergütz, L., Novais, R. F., Marciano da Costa, L., Pinto, F. G., Tronto, J.,  
450 2015. Layered double hydroxides: nanomaterials for applications in agriculture, *R. Bras. Ci.*  
451 *Solo.* 39, 1-13.

452 Betega de Paiva, L., Morales, A. R., Valenzuela Díaz, F.R., 2008. Organoclays: Properties,  
453 preparation and applications. *Applied Clay Science.* 42, 8–24.

454 Bish, D.L., 1980. Anion exchange in takovite: application to other hydroxide minerals. *Bull.*  
455 *Mineral.* 103, 170–175.

456 Bujdosó, T., Patzkó, Á., Galbács, Z., Dékány, I., 2009. Structural characterization of arsenate  
457 ion exchanged MgAl-layered double hydroxide. *Applied Clay Science* 44, 75–82.

458 Cavani, F., Trifiro, F., Vaccari, A., 1991. Hydrotalcite-type anionic clays: preparation,  
459 properties and applications. *Catal. Today* 11, 173–301.

460 Chiu, C.-W., Huang, T.-K., Wang, Y.-C., Alamani, B. G., Lin, J.-J., 2014. Intercalation  
461 strategies in clay/polymer hybrids. *Progress in Polymer Science.* 39, 443–48.

462 Choy J.-H., Jung, J.-S., Oh, J.-M., Park, M., Jeong, J., Kang, Y.-K., Han, O.-J. 2004. Layered  
463 double hydroxide as an efficient drugreservoir for folate derivatives. *Biomaterials* 25, 3059-  
464 3064.

465 Choy, J.-H., Choi, S.-J., Oh, J.-M., Park, T., 2007. Clay minerals and layered double  
466 hydroxides for novel biological applications. *Applied Clay Science.* 36, 122–132.

467 Constantino, U., Nocchetti, M., 2001. Layered Double Hydroxides and Their Intercalation  
468 Compounds in Photochemistry and Medicinal Chemistry. In: Rives, V. (Ed); *Layered Double*  
469 *Hydroxides: Present and Future*, Nova Science Publishers: New York, pp. 383–412.

470 Costa, F. R., Leuteritz, A., Wagenknecht, U., Jehnichen, D., Häußler, L., Heinrich, G., 2008.  
471 Intercalation of Mg–Al layered double hydroxide by anionic surfactants: Preparation and  
472 characterization. *Applied Clay Science*. 38, 153–164.

473 Costa, P., Lobo, J. M. S., 2001. Modeling and comparison of dissolution profiles. *European*  
474 *Journal of Pharmaceutical Sciences* 13, 123–133.

475 Cunha, A. S., Grossiord, J. L., Puisieux, F., Seiller, M., 1997. Insulin in w/o/w multiple  
476 emulsions: preparation, characterization and determination of stability towards proteases in  
477 vitro. *J. Microencapsul.* 14, 311–319.

478 Cunha, V. R. R., Barbosa de Souza, R., Rebello Pinto da Fonseca Martins, A. M. C., Koh, I.  
479 H. J., Leopoldo Constantino, V. R., 2016. Accessing the biocompatibility of layered double  
480 hydroxide by intramuscular implantation: histological and microcirculation evaluation. *Nature*  
481 *Scientific reports*. DOI: 10.1038/srep30547.

482 Deák, Á., Janovák, L., Tallósy, Sz. P., Bitó, T., Sebők, D., Buzás, N., Pálinkó, I., Dékány, I.,  
483 2015. Spherical LDH–Ag<sup>0</sup>-Montmorillonite Heterocoagulated System with a pH-Dependent  
484 Sol–Gel Structure for Controlled Accessibility of AgNPs Immobilized on the Clay Lamellae.  
485 *Langmuir*. 31, 2019–2027.

486 Deák, Á., Janovák, L., Csapó, E., Ungor, D., Pálinkó, I., Puskás, S., Ördög, T., Ricza, T.,  
487 Dékány, I., 2016. Layered double oxide (LDO) particle containing photoreactive hybrid layers  
488 with tunable superhydrophobic and photocatalytic properties. *Applied Surface Science* 389,  
489 294–302.

490 Deng, L., Shi, Z., Xiaoxu Peng, X. 2015. Adsorption of Cr(VI) onto a magnetic CoFe<sub>2</sub>O<sub>4</sub>/  
491 MgAl-LDH composite and mechanism study. *RSC Adv.*, 5, 49791–49801.

492 Frenning, G., 2011. Modelling drug release from inert matrix systems: From moving-  
493 boundary to continuous-field descriptions. *International Journal of Pharmaceutics* 418, 88–99.

494 Fudala, Á., Pálinkó, I., Kiricsi, I., 1999. Amino acids, precursors for cationic and anionic  
495 intercalation synthesis and characterization of amino acid pillared materials. *J. Mol. Struct.*  
496 482-483, 33–37.

497 Geng, W., Nakajima, T., Takanashi, H., Akira Ohki, A., 2009. Analysis of carboxyl group in  
498 coal and coal aromaticity by Fourier transform infrared (FT-IR) spectrometry. *Fuel*. 88, 139–  
499 144.

500 Glavin, G. B., Bose, R., Pinsky, C., 1989. Kynurenic acid protects against gastroduodenal  
501 ulceration in mice injected with extracts from poisonous atlantic shellfish. *Prog. Neuro-*  
502 *Psychopharmacol.* 6 *Biol. Psychiat.* 13, 569-572.

503 Glavin, G. B., Pinsky, C., 1989. Kynurenic acid attenuates experimental ulcer formation and  
504 basal gastric acid secretion in rats. *Res Commun Chem Pathol Pharmacol.* 64 (1), 111-119.

505 Goh, K.-H., Lim, T.-T., Dong, Z.L., 2008. Application of layered double hydroxides for  
506 removal of oxyanions: A review. *Water Res.* 42, 1343–1368.

507 Guérin, D., Vuilleumard, J.-C., Subirade, M., 2003. Protection of Bifidobacteria Encapsulated  
508 in Polysaccharide-Protein Gel Beads against Gastric Juice and Bile. *Journal of Food*  
509 *Protection*, 66 (11), 2076–2084

510 Ibrahim, M., Nada, A., Kamal, D. E., 2005. Density functional theory and FTIR spectroscopic  
511 study of carboxyl group. *Indian Journal of Pure & Applied Physics.* 43, 911-917.

512 **Joshi, G. V., Patel, H. A., Bajaj, H. C., Jasra, R. V. 2009. Intercalation and controlled release**  
513 **of vitamin B6 from montmorillonite–vitamin B6 hybrid. *Colloid Polym Sci* 287, 1071–1076.**

514 Juhász, Á., Csapó, E., Ungor, D., Tóth, G. K., Vécsei, L., Dékány, I., 2016. Kinetic and  
515 Thermodynamic Evaluation of Kynurenic Acid Binding to GluR1270–300 Polypeptide by  
516 Surface Plasmon Resonance Experiments. *J. Phys. Chem. B.* 120, 7844–7850.

517 **Kevadiya, B. D., Joshi, G. V., Patel, H. A., Ingole, P. G., Mody, H. M., Bajaj, H. C. 2010.**  
518 **Montmorillonite-Alginate Nanocomposites as a Drug Delivery System: Intercalation and In**

519 Vitro Release of Vitamin B<sub>1</sub> and Vitamin B<sub>6</sub>. *Journal of biomaterials applications* 25 (2), 161-  
520 177.

521 Li, B., He, J., Evans, D.G., Duan, X., 2004. Inorganic layered double hydroxides as a drug  
522 delivery system-intercalation and in vitro release of fenbufen. *Appl. Clay Sci.* 27, 199–207.

523 López, T., Ortiz, E., Gómez, E., Pérez-de la Cruz, V., Carrillo-Mora, P., Novaro, O., 2014.  
524 Preparation and Characterization of Kynurenic Acid Occluded in Sol-Gel Silica and SBA-15  
525 Silica as Release Reservoirs. *Journal of Nanomaterials*. 2014, 8.

526 Marosi, M., Nagy, D., Farkas, T., Kis, Z., Rózsa, É., Robotka, H., Fülöp, F., Vécsei, L., Toldi,  
527 J., 2010. A novel kynurenic acid analogue: a comparison with kynurenic acid, An in vitro  
528 electrophysiological study. *J. Neural. Transm.* 117, 183–188.

529 Nagy, K., Bíró, G., Berkesi, O., Benczédi, D., Ouali, L., Dékány, I., 2013. Intercalation of  
530 lecithins for preparation of layered nanohybrid materials and adsorption of limonene. *Applied*  
531 *Clay Science*. 72, 155–162.

532 Oh, J.-M., Choi, S.-J., Kim, S.-T., Choy, J.-H., 2006. Cellular uptake mechanism of an  
533 inorganic nanovehicle and its drug conjugates: Enhanced efficacy due to clathrin-mediated  
534 endocytosis. *Bioconjug. Chem.* 17, 1411–1417.

535 Oh, M.-J., Biswick, T. T., Choy, J.-H., 2009. Layered nanomaterials for green materials. *J.*  
536 *Mater. Chem.* 19, 2553–2563.

537 Patzkó, Á., Kun, R., Hornok, V., Dékány, I., Engelhardt, T., Schall, N., 2005. ZnAl-layer  
538 double hydroxides as photocatalysts for oxidation of phenol in aqueous solution. *Colloids and*  
539 *Surfaces A: Physicochem. Eng. Aspects* 265, 64–72.

540 Peppas, N. A., Merrill, E. W., 1977. Crosslinked Poly( vinyl Alcohol) Hydrogels as Swollen  
541 Elastic Networks, *Journal of Applied Polymer Science* 21, 1763-1770.



542 Patel, H. A., Shah, S., Shah, D. O., Joshi, P. A. 2011. Sustained release of venlafaxine from  
543 venlafaxine–montmorillonite–polyvinylpyrrolidone composites. *Applied Clay Science* 51,  
544 126–130.

545 Pietrzyńska, M., Voelkel, A., 2017. Stability of simulated body fluids such as blood plasma,  
546 artificial urine and artificial saliva. *Microchemical Journal*. 134, 197–201.

547 Posati, T., Bellezza, F., Tarpani, L., Perni, S., Latterini, L., Marsili, V., Cipiciani, A., 2012.  
548 Selective internalization of ZnAl–HTlc nanoparticles in normal and tumor cells. A study of  
549 their potential use in cellular delivery. *Appl. Clay Sci.* 55, 62–69.

550 Siepmann, J., Peppas, N. A., 2011. Higuchi equation: Derivation, applications, use and  
551 misuse, *International Journal of Pharmaceutics* 418, 6–12.

552 Szabó, T., Veres, Á., Cho, E., Khim, J., Varga, N., Dékány, I., 2013. Photocatalyst separation  
553 from aqueous dispersion using graphene oxide/TiO<sub>2</sub> nanocomposites. *Coll. Surf. A.* 433,  
554 230–239.

555 Tarnawski, A.S., Tomikawa, M., Ohta, M., Sarfeh, I.J., 2000. Antacid talcid activates in  
556 gastric mucosa genes encoding for EGF and its receptor. The molecular basis for its ulcer  
557 healing action. *J. Physiol., Paris* 94, 93–98.

558 Trifiro, F., Vaccari, A., 1996. Hydrotalcite-like anionic clays (layered double hydroxides).  
559 *Compr. Supramol. Chem.* 7, 251–291.

560 Turski, M. P., Turska, M., Paluszkiewicz, P., Parada-Turska, J., Oxenkrug, G. F., 2013.  
561 Kynurenic Acid in the Digestive System—New Facts, New Challenge. *International Journal*  
562 *of Tryptophan Research.* 6, 47–55.

563 Varga, N., Csapó, E., Majláth, Z., Ilisz, I., Krizbai, I. A., Wilhelm, I., Knappe, L., J. Toldi, J.,  
564 Vécsei, L., Dékány I., 2016. Targeting of the kynurenic acid across the blood–brain barrier by  
565 core-shell nanoparticles. *European Journal of Pharmaceutical Sciences* 86, 67–74.

566 Yang, J.H., Lee, S.Y., Han, Y.S., Park, K.C., Choy, J.H., 2003. Efficient transdermal  
567 penetration and improved stability of L-ascorbic acid encapsulated in an inorganic  
568 nanocapsule. Bull. Korean Chem. Soc. 24, 499–503.  
569

570 **Figure 1.** PXRD pattern of the synthesized 2:1 Mg/Al LDH powder (a) and the charge  
571 titration curve of 0.1 wt.% cationic LDH suspension (pH=10) with 0.1 wt.% of anionic  
572 sodium dodecyl sulfate (NaDS) surfactant solution (b).

573 **Figure 2.** Adsorption isotherms of N<sub>2</sub> at 77 K on LDH powder sample (a). The inserted figure  
574 shows the corresponding deBoer *t*-plot of the same sample (b).

575 **Figure 3.** The effect of the KYNA weight ratio on the intercalation capacity of the KYNA  
576 molecules loaded LDH layers

577 **Figure 4.** PXRD patterns of the initial LDH lamellae and KYNA molecules intercalated into  
578 the LDH layers and the proposed structure of KYNA-LDH composite

579 **Figure 5.** FT-IR spectra for (a) LDH drug carrier, (b) KYNA-LDH composite and (c) KYNA  
580 powder samples

581 **Figure 6.** TG profiles for LDH drug carrier, KYNA-LDH composite and initial KYNA

582 **Figure 7.** The gravimetrically measured percentage weight loss of the LDH drug carrier in  
583 ~~SGJ~~ SGF media at pH= 1.5 (a) and the corresponding PXRD patterns of LDH sample during  
584 the dissolution process (b).

585 **Figure 8.** The percentage release profile of anionic KYNA molecules at two different pH  
586 values (pH= 6.70 and 1.50) and the KYNA release from LDH lamellae at acidic (pH= 1.50)  
587 pH, as well as the measured KYNA concentration values (C<sub>t</sub>, mg/ mL) as a function of release  
588 time with the fitted curves calculated by the first-order rate model

589 **Table 1.** Interpretation of the release experiments using different various models.

1 **Anti-ulcerant kynurenic acid molecules intercalated Mg/Al-layered double hydroxide**  
2 **and its release study**

3  
4 Ágota Deák<sup>a</sup>, Edit Csapó<sup>a,b</sup>, Ádám Juhász<sup>a,b</sup>, Imre Dékány<sup>a,b</sup>, László Janovák<sup>a,\*</sup>

5 *<sup>a</sup>Department of Physical Chemistry and Materials Science, University of Szeged, H-6720,*  
6 *Szeged, Rerrich B. tér 1, Hungary*

7 *<sup>b</sup>MTA-SZTE Biomimetic Systems Research Group, University of Szeged, H-6720, Szeged,*  
8 *Dóm tér 8, Hungary*

9  
10 \* Corresponding authors. Tel.: +36 62 544 210; Fax: +36 62 544 042.

11 *E-mail address: [janovaki@chem.u-szeged.hu](mailto:janovaki@chem.u-szeged.hu) (L. Janovák)*

12  
13  
14 **Abstract**

15 Kynurenic acid (KYNA) is a product of the tryptophan metabolism and it possess also anti-  
16 ulcerant properties, however, the application of KYNA for the treatment of gastroduodenal  
17 ulceration is limited, because the concentration of KYNA is very low in human gastric fluid  
18 (0.01  $\mu\text{M}$ ). The intercalation of KYNA molecules into biocompatible Mg–Al layered double  
19 hydroxides (LDH) lamellae could solve this problem. For this purpose Mg–Al LDH with  
20  $114.96 \pm 0.48 \text{ m}^2/\text{g}$  BET surface area and +0.641 meq/g specific surface charge was  
21 synthesized. The intercalation of the anionic target molecules into positively charged LDH  
22 layers was carried out with simply ion- exchange reaction. The structure of the obtained  
23 KYNA/ LDH hybrid materials were studied by powdered X-ray diffraction (PXRD) and  
24 Attenuated total reflection Fourier transform infrared (ATR-FTIR) spectroscopy verifying that  
25 the KYNA molecules prefer creating a paraffin type monolayer arrangement. Due to the

26 intercalation process the (003) reflection peaks of initial LDH ( $2\Theta= 11.39^\circ$ ,  $d_{(003)}= 0.775$  nm)  
27 shift to lower angles ( $2\Theta= 4.11^\circ$ ,  $d= 2.146$  nm). That means, that the basal space value ( $\Delta d_L$ )  
28 of the KYNA-LDH sample was 1.436 nm. The total amount of the intercalated KYNA  
29 molecules into LDH layers was measured by fluorescence spectroscopy method. According to  
30 the results the drug- loading capacity was about 120 mg KYNA/ g LDH. This ~12% KYNA  
31 content of the hybrid materials was also evidenced by thermogravimetric measurements,  
32 because the thermal decomposition of the bio-hybrid materials was examined by  
33 thermogravimetry (TG) analysis. Our experimental data confirm that the anti- ulcerant KYNA  
34 molecules can be safely loaded and stored into LDH's layers forming a new bio-active hybrid  
35 material. In addition we also presented by PXRD and gravimetric measurements that prepared  
36 LDH layers were almost completely dissolved (~83 wt.%) in the applied simulated gastric  
37 fluid (SGF) media (pH=1.5) under 60 min and the encapsulated KYNA molecules released  
38 from the destroyed interlayers. Finally, the measured KYNA drug release profile from the  
39 bioactive composite material was also presented in SGF media. According to the results 18%  
40 of the loaded KYNA molecules were released during 6 hours.

41

42 **Keywords:** layered double hydroxide, kynurenic acid, intercalation, *in vitro* drug release  
43 study, anti- ulcerant properties, simulated gastric fluid

44

## 45 1. Introduction

46 LDHs are a class of anionic lamellar compounds made up of positively charged brucite- like  
47 layers (Trifiro and Vaccari, 1996). The chemical composition of the two layers of  
48 hydrotalcite-type minerals can be given by the following general formula:  
49  $[M^{2+}_{1-x}M^{3+}_x(OH)_2]^{b+} \cdot [A_{b/n}]^{n-} \cdot mH_2O$ , where  $M^{2+}$  represents divalent and  $M^{3+}$  represents  
50 trivalent cations, the value of x may vary in the range of 0.2–0.4, and A is the anion among

51 the cationic layers ( $\text{OH}^-$ ,  $\text{Cl}^-$ ,  $\text{NO}_3^-$ ,  $\text{CO}_3^{2-}$ , and  $\text{SO}_4^{2-}$ ) (Constantino and Nocchetti, 2001).  
52 LDHs have been widely exploited to create new materials for applications in catalysis (Patzkó  
53 et al., 2005; Deák et al., 2016), drug delivery and environmental remediation (Bujdosó et al.,  
54 2009; Goh et al., 2008). MgAl-LDHs are most frequently used as a LDH-based drug carrier  
55 and as evidence of its low toxicity, it is widely used as an antacid (Tarnawski et al., 2000) and  
56 the biocompatibility of this layered material was also reported in the literature (Cunha et al.,  
57 2016, Nagy et al., 2013). LDHs particularly prefer multivalent anions within their interlayer  
58 space due to strong electrostatic interaction and therefore LDHs bearing monovalent anions  
59 like nitrate or chloride ions are good precursors for exchange reactions (Choy et al., 2007).  
60 The solubility and surface charge of LDHs as hydroxides is highly pH-dependent (Bish, 1980;  
61 Deák et al., 2015).

62 Layered clay minerals are widely used for their capability to intercalate molecules in the  
63 interlayer space. It is also well known that beside the LDH drug carrier, the negatively  
64 charged clay minerals such as Montmorillonite  $[(\text{Na,Ca})_{0.33}(\text{Al, Mg})_2(\text{Si}_4\text{O}_{10})(\text{OH})_2 \cdot n\text{H}_2\text{O}]$   
65 exhibit an excellent sorption property, large specific surface area, cation exchange capacity  
66 and drug-carrying capability (Joshi et al., 2009; Patel et al., 2011; Kevadiya et al., 2010). It is  
67 worth mentioning that the pioneering works of Choy' group have led to a rapid development  
68 in the research on both varied LDHs/polymers/anions hybrid systems and pharmaceutical  
69 applications of LDHs especially involving the biocompatibility and toxicity of LDHs and  
70 anti-cancer drugs intercalated LDH materials (Choy et al., 2007). Li et al. also developed anti-  
71 inflammatory drug fenbufen-LDH hybrids and showed that these drug-inorganic hybrid  
72 materials can be used as an effective drug delivery system due to their controlled release  
73 capacity (Li et al., 2004). Yang et al. reported the intercalation of vitamins A, E, and C into  
74 LDHs (Yang et al., 2003). Moreover, in addition to the intercalation of pharmaceutical drugs  
75 into layered materials causing no significant denaturation of the drug molecules, it has also

76 been shown to enhance the internalization of the drug into a target cell without any noticeable  
77 side effects (Oh et al., 2009). Thus, LDHs can not only play a role as a biocompatible-  
78 delivery matrix for drugs but also afford a significant increase in the delivery efficiency  
79 (Posati et al., 2012; Oh et al., 2006).

80 Kynurenic acid (KYNA) is a product of the tryptophan metabolism, it has a neuroprotective  
81 and neuroinhibitory properties (Marosi et al., 2010). According to this the interactions  
82 between the different model peptide fragment of human glutamate receptor and KYNA  
83 molecules has relevance in neuroscience (Juhász et al., 2016). Moreover, experimental data  
84 indicate that KYNA may be neuroprotective and it may be of therapeutic value for several  
85 neurological disorders (Varga et al., 2016). Some article also reported that the KYNA may  
86 prove useful against domoic acid induced gastropathy because it protects against  
87 gastroduodenal ulceration (Glavin et al., 1989a). Furthermore, it was also reported that  
88 KYNA protects against gastric and duodenal ulceration caused by a poisonous Atlantic  
89 shellfish (Glavin and Pinsky, 1989b). However, according to the publication of Turski et. al.,  
90 the concentration of KYNA increases gradually along the gastrointestinal tract, reaching its  
91 highest value at the very end of it and the lowest concentration of KYNA was found in human  
92 gastric juice (0.01  $\mu\text{M}$ ) (Turski et al., 2013). Thus, the application of KYNA for the treatment  
93 of gastroduodenal ulceration is limited.

94 Numerous mathematical models (zero-order, first-order, Weibull, Hixone-Crowell,  
95 Korsmeyere-Peppas, etc) have been developed to describe the release properties of the drug  
96 molecules (Costa and Lobo, 2001). There has not been reported mathematical model in the  
97 literature that takes into account all the important effects, in this way we chose three models  
98 that are widely used in literature. The first-order rate model is a typically used model which  
99 describes the adsorption and/or elimination of certain drugs and states that the drug release  
100 rate depends on its concentration.

101  $C_t = C_0 e^{-kt}$  (1)

102 where  $C_0$  is the initial concentration of drug in the drug formulation,  $C_t$  is the concentration of  
103 drug in the drug formulation at time  $t$ , and  $k$  is the first-order release constant with units of  
104 reciprocal time.

105 Presently, many authors utilize the semi-empirical power law model that was proposed by  
106 Korsmeyer and Peppas (Peppas and Merrill, 1977). The model was developed to specifically  
107 model the release of a drug molecule from a polymeric matrix, such as a hydrogel using the  
108 following equation:

109  $C_t = C_0 k_m t^n$  (2)

110 where  $C_0$  is the initial concentration of drug in the drug formulation,  $C_t$  is the concentration of  
111 released drug at time  $t$ ,  $k_m$  is the kinetic constant and  $n$  the release index, indicating the  
112 mechanism of the drug release. At  $n > 0.45$ , non Fickian diffusion is observed, while  $n \leq 0.45$   
113 represents the Fickian diffusion mechanism. The  $n$  values refer to the geometries of the  
114 particles; in the diffusion-controlled release if the value of  $n$  is between 0.45 and 0.43, the  
115 geometries are slab, cylinder or sphere, respectively.

116 Many times the drug release process can be modeled with the classical Fick's diffusion  
117 equation or with the simplified Higuchi expressions (Siepmann and Peppas, 2011). Higuchi  
118 was the first in 1961 who described the release of the drug from an insoluble matrix based on  
119 Fickian diffusion. The Higuchi model is valid for the systems where the initial drug  
120 concentration in the matrix is much higher than the solubility of the drug.

121  $C_t = k_H \sqrt{t}$  (3)

122 where  $C_t$  is the concentration of drug in the drug matrix at time  $t$  and  $k_H$  is the Higuchi  
123 dissolution constant.

124 In this article the intercalation of neuroprotective and anti- ulcerant KYNA molecules in the  
125 biocompatible MgAl-LDH drug carrier system was examined. The quantitative



126 characterization of intercalation and the structural properties of the prepared KYNA pillared  
127 LDH composite materials was also reported. In addition, the LDH dissolution and the KYNA  
128 drug release profile from the bioactive composite material was also presented in simulated  
129 gastric fluid (SGF).

130

## 131 **2. Materials and methods**

### 132 2.1. Reagents

133 For the synthesis of layered double hydroxides magnesium nitrate hexahydrate  
134 ( $\text{Mg}(\text{NO}_3)_2 \cdot 6\text{H}_2\text{O}$ , 98%; Sigma-Aldrich, United Kingdom), and aluminum nitrate nonahydrate  
135 ( $\text{Al}(\text{NO}_3)_3 \cdot 9\text{H}_2\text{O}$ , 99.7%; Molar Chemicals Kft., Hungary) were used as precursors.  
136 Kynurenic acid (KYNA) was obtained from Sigma-Aldrich, United Kingdom. The sodium  
137 dodecyl sulfate ( $\text{C}_{12}\text{H}_{25}\text{NaO}_4\text{S}$ , 98%), hydrochloric acid (HCl, 37%) were obtained from  
138 Molar Chemicals Kft., Hungary. The pH was adjusted with sodium hydroxide (NaOH,  
139 99.80%) and hydrochloric acid (HCl, 37%) which were obtained from Molar Chemicals Kft.,  
140 Hungary. The SGF media was prepared using pepsin (1:10000 NF; 2000 u/g activity) and  
141 hydrochloric acid (HCl, 37%) obtained from Molar Chemicals Kft., Hungary and potassium  
142 chloride (KCl, 99.5-100%) obtained from Reanal, Hungary. Furthermore, sodium chloride  
143 ( $\text{NaCl}$ , 99.98%), sodium phosphate dibasic dodecahydrate ( $\text{Na}_2\text{HPO}_4 \cdot 12\text{H}_2\text{O}$ , 100.3%) and  
144 sodium dihydrogen phosphate monohydrate ( $\text{NaH}_2\text{PO}_4 \cdot \text{H}_2\text{O}$ , 99%) were obtained from Molar  
145 Chemicals Kft., Hungary and were used for preparing PBS buffer. All aqueous solutions were  
146 made using deionized water.

147

### 148 2.2. Synthesis of 2:1 Mg/Al-LDH

149 Mg/Al-LDH was synthesized by co-precipitation method under  $\text{N}_2$  atmosphere to avoid or at  
150 least to minimize the contamination of LDH by atmospheric  $\text{CO}_2$ , because the adsorption

151 affinity of the carbonate anions derived from atmospheric CO<sub>2</sub> is very high for LDH (Choy et  
152 al., 2004). So, in the case of the carbonation of the LDH, the further intercalation and ion-  
153 exchange of the CO<sub>3</sub>- LDH would be impossible. During the synthesis 25.64 g of Mg(NO<sub>3</sub>)<sub>2</sub> ·  
154 6 H<sub>2</sub>O and 18.76 g of Al(NO<sub>3</sub>)<sub>3</sub> · 9H<sub>2</sub>O were dissolved in 300 mL of distilled water under  
155 vigorous stirring and nitrogen atmosphere at room temperature. The molar ratio of Mg:Al was  
156 2:1. Then, 200 mL of 1.875 mol/L concentration of NaOH was added dropwise to the first  
157 solution to obtain the pH=13. The resulting mixture was vigorously stirred at 80°C  
158 temperature under nitrogen atmosphere for 17 hours and aged at 80°C for 3 days. The  
159 resulting precipitate was separated by centrifugation, washed with distilled water twice and  
160 dried in an oven at 60°C overnight.

161

### 162 2.3. Intercalation of KYNA molecules into LDH layers

163 First, the KYNA/LDH weight ratio was systematically changed in order to determine the  
164 maximal intercalation capacity of the LDH layers for the KYNA drug molecules. During this  
165 experiments a calibration series was made from 2 mM KYNA stock solution using double  
166 dilutions and the KYNA concentration was determined by fluorometric measurements. The  
167 fluorescence spectra were recorded by a Horiba Jobin Yvon Fluoromax-4 spectrofluorometer  
168 (excitation at  $\lambda = 350$  nm). The KYNA concentration was quantified by the determined  
169 spectrofluorometric calibration curve between 355-550 nm emission wavelength range and at  
170 a wavelength maximum of  $\lambda_{\max} = 380$  nm. During the adsorption measurements, the KYNA  
171 weight ratio was 0; 0.025; 0.05; 0.1; 0.165; 0.3 0.5 referred to the LDH host lamellae. The  
172 prepared KYNA/LDH suspensions were stirred for 1 hour at room temperature (25 ° C) in  
173 order to reach the adsorption equilibrium, then were filtered through a fine filter (Millipor,  
174 0.22  $\mu\text{m}$ ) than the KYNA concentration was determined from the spectrofluorometric

175 calibration curves. The experiments were carried out triplicate, and average values are  
176 reported. Error bars refer to the standard deviation.

177 In the continuation, the amount of intercalated anionic substance (KYNA) was set at 30 wt%  
178 based on the LDH mass, i.e. the anionic KYNA/LDH weight ratio was 300 mg KYNA / g  
179 LDH. During the intercalation, 30 mg of KYNA was added to 10 ml of 1 wt% LDH  
180 suspension and stirred at 25°C for 48 hours under a nitrogen atmosphere to avoid the  
181 contamination of LDH by atmospheric CO<sub>2</sub>. The pH of the LDH suspensions was adjusted to  
182 10.0 by dropwise addition of 1 mol/L concentration of NaOH solution. The reaction product  
183 was filtered, washed with distilled water to remove adhered KYNA molecules, and dried at 60  
184 °C in an oven for 24 h.

185

## 186 2.4. Methods of sample characterization

### 187 2.4.1. *PXRD measurements*

188 The X-ray diffractograms of the powdered 2:1 Mg/Al-LDH and the KYNA intercalated LDH  
189 layers were recorded on a Philips X ray diffractometer (PXRD) with CuK<sub>α</sub> (= 0.1542 nm) as  
190 the radiation source at ambient temperature in the 2–40° and 2.5–15° (2 $\Theta$ ) range applying  
191 0.02° (2 $\Theta$ ) step size.

192

### 193 2.4.2. *Determination of surface charge of LDH samples*

194 The surface charges of the LDH samples were measured in a particle charge detector (PCD-  
195 02 MÜTEK) with manual titration. In the course of a titration process, the surface charges of  
196 the studied samples were compensated by oppositely charged sodium dodecyl sulfate (SDS)  
197 surfactants with concomitant streaming potential measurements. During the titration process,  
198 10 mL of a 0.1% LDH (pH=10) was added to the test cell of the PCD, and was titrated with  
199 oppositely charged surfactant (SDS) solution. The equimolar amount of surfactant was

200 calculated from the surfactant amounts added at the charge compensation point (where  
201 streaming potential = 0 mV) and was normalized to the amount of titrated sample (meq/g).

202

#### 203 2.4.3. *Determination of specific surface area of LDH sample (BET measurement)*

204 The specific surface area of the LDH sample was determined by BET method from N<sub>2</sub>  
205 adsorption isotherms at  $77 \pm 0.5$  K (Micromeritics Gemini 2375 Surface Area Analyzer).  
206 Before the adsorption measurements the samples were evacuated ( $10^{-5}$  mmHg) at 100°C  
207 overnight.

208

#### 209 2.4.4. *ATR-FTIR spectroscopy measurements*

210 Attenuated total reflection Fourier transform infrared (ATR-FTIR) spectroscopy  
211 measurements were performed by a Biorad FTS-60A FT-IR spectrometer by accumulation of  
212 256 scans at a resolution of  $4\text{ cm}^{-1}$  between  $4000$  and  $500\text{ cm}^{-1}$ . Each sample was previously  
213 weighted before spectrum acquisition (about  $10 \pm 1$  mg of powder sample) and placed onto  
214 the ATR crystal. All spectral manipulations were performed using Thermo Scientific  
215 GRAMS/AI Suite software.

216

#### 217 2.4.5. *TG measurements*

218 The thermal behavior of the LDH drug carrier, KYNA/LDH composite and KYNA and the  
219 KYNA content of the composite were investigated with thermogravimetric (TG) analysis.  
220 During TG measurements, the samples were heated in synthetic air from 25 to 1000°C at a  
221 heating rate of 5°C/min (Mettler-Toledo TGA/SDTA 851<sup>e</sup> Instrument).

222

223 2.5. Dissolution experiment of LDH in acidic SGF media

224 The dissolution process of the LDH drug carrier was investigated in the presence of the  
225 simulated gastric fluid (SGF) at pH= 1.5 which was prepared with a buffer mixture composed  
226 of 0.2 M HCl solution and 0.2 M KCl solution, to which pepsin was added at a ratio of 10  
227 U/ml (Guérin et al., 2003; Cunha et al., 1997). During the process 1.491 g of KCl and 0.5 g of  
228 pepsin were dissolved in 100 mL of distilled water under vigorous stirring and 1.67 mL of  
229 37% concentration of HCl was added dropwise to the SGF solution to obtain the pH at 1.5.  
230 Then, 1.0 g of LDH powder sample was added to the SGF solution. The concentration of  
231 LDH in SGF solution was 0.01 g/mL. The dissolution of LDH was followed by  
232 gravimetrically measurements and the degradation of LDH was also recorded with PXRD  
233 measurements (using Philips X ray diffractometer with  $\text{CuK}_\alpha$  ( $\lambda = 0.1542$  nm) as the radiation  
234 source at ambient temperature in the  $2\text{--}30^\circ$  ( $2\theta$ ) range applying  $0.02^\circ$  ( $2\theta$ ) step size.). The  
235 weight- loss measurements were carried out triplicate, and average values are reported with  
236 the calculated standard deviations.

237

238 2.6. In vitro drug release experiments

239 The in vitro experiments were carried out using a dialysis tubing cellulose membrane (typical  
240 molecular weight cut-off= 12-14 kDa from Sigma Aldrich). Briefly, 1 mL of KYNA solution  
241 ( $c = 1.6$  mg/mL) or KYNA/LDH dispersion in PBS buffer ( $c = 1.6$  mg/mL, KYNA content:  
242  $\sim 12\%$ ), (pH=6.70) was pipetted into the tube membrane ( $d = 1$  cm,  $l = 10$  cm) then immersed  
243 into 100 mL of PBS solution (at pH= 6.70 and 1.50) in a vertical position. The 100 mL of  
244 PBS solution with the carefully closed membrane was stirred continuously with a magnetic  
245 stirrer and the release experiments were carried out at  $37.0^\circ\text{C}$  using a water bath. Samples  
246 were taken every 2.5 minutes in the first 10 minutes, then were taken in the 15<sup>th</sup> and 20<sup>th</sup>  
247 minutes. After 20 minutes the samples were taken in each 10 minutes until the first hour and

248 then were taken after 30 minutes in every hour. Measurements were performed in 240 min.  
249 The presence of kynurenic acid was recorded with a diode array spectrophotometer (Ocean  
250 Optics USB2000; USA) in the  $\lambda = 250\text{--}350$  nm range using a 1 cm quartz cuvette. The  
251 released kynurenic acid concentration was quantified by the previously determined  
252 spectrophotometric calibration curve at a wavelength maximum of  $\lambda_{\text{max}} = 311$  nm. To  
253 determine the value of kinetic constants of the applied release kinetic models, the sum of the  
254 square of differences between the measured and predicted concentration values have been  
255 minimalized using a spreadsheet based computer application for nonlinear parameter  
256 estimation (Juhász et al., 2016).

257

### 258 **3. Results and discussion**

#### 259 3.1. Characterization of the 2:1 Mg/Al-LDH

260 Fig. 1a illustrates the PXRD pattern of the synthesized Mg/Al-LDH sample and displays the  
261 (003) and (006) Bragg reflections characteristic to layered double hydroxides (JCPDS No. 89-  
262 0460) (Deng et al., 2015). These peaks are positioned at an angle of  $11.39^\circ$  ( $2\Theta$ ) ( $d_{(003)} = 0.77$   
263 nm) and the peak representing the secondary reflection is at an angle of  $22.82^\circ$  ( $2\Theta$ ) ( $d_{(006)} =$   
264 0.39 nm). In addition, further characteristic reflection was observed at angle of  $34.39^\circ$  ( $2\Theta$ )  
265 ( $d_{(009)} = 0.26$  nm) which is the (009) reflection characteristic to the sample (Costa et al.,  
266 2008). The surface charge value of LDH was determined by charge titration (Szabó et al.,  
267 2013). The streaming potentials of diluted, 0.1 wt.% LDH suspension (pH=10) was measured  
268 in a Műtek PCD02 apparatus, while adding oppositely charged NaDS surfactant solution to  
269 the system. A typical charge titration curve is presented in Fig. 1b. The measured initial  
270 streaming potential of layered LDH was positive (+704 mV). This value gradually decreased  
271 upon addition of the oppositely charged 0.1% anionic SDS solution, and reached 0 mV after  
272 the addition of 1.8 ml of surfactant solution. At this point (i.e., the charge equivalence point or

273 c.e.p.), the negatively charged anionic surfactant molecules compensated the positive charge  
274 of LDH in the aqueous suspension. Due to the surface adsorption of the SDS molecules on the  
275 hydrophilic LDH lamellae, the obtained hydrophobized sample was sedimented from the  
276 aqueous media after the titration process (see inserted photos). Based on the charge titration  
277 data, the specified charge of LDH at pH= 10 was +0.641 meq/g LDH. The positive surface  
278 charge of conventional LDH layers of lamellar structure is well-known in the literature  
279 (Glavin et al., 1989a), and creates the basis of its widespread utilization for the adsorption of  
280 various negatively charged molecules (Choy et al., 2007; Fudala et al., 1999).

281 The BET adsorption isotherm of the LDH sample reveals type II isotherm, expressing  
282 multilayer N<sub>2</sub> adsorption, without significant hysteresis loops between the adsorption and  
283 desorption branches (Fig. 2a). The analysis of the N<sub>2</sub> adsorption isotherm by the t-plot method  
284 (Fig. 2b, inset) shows that the sample has a nonporous structure. The BET- method was used  
285 to calculate the surface area of the LDH which was  $114.96 \pm 0.48 \text{ m}^2/\text{g}$ .

286

### 287 3.2. Characterization of the intercalated kynurenic acid in LDH drug carrier

288 The prepared positively charged (+0.641 meq/g) LDH lamellae with relatively high specific  
289 surface area ( $114.96 \pm 0.48 \text{ m}^2/\text{g}$ ) was suitable for the intercalation of negatively charged  
290 guest molecules. The intercalation capacity of the KYNA drug molecules into LDH layers  
291 was measured by fluorescence spectroscopy method (Fig. 3). During the experiments, the  
292 KYNA content of the samples was systematically changed from 2.5 to 50 wt.%. The obtained  
293 results presented in Fig. 3 showed that with the increasing weight ratio of KYNA/LDH the  
294 amount of intercalated KYNA is also increasing and the determined drug- loading capacity  
295 was about 120 mg KYNA/ g LDH. Considering that the measured surface charge of LDH was  
296 +0.641 meq/g LDH and the molecular weight of KYNA (189.16 g/mol), the calculated

297 theoretical intercalated amount of KYNA was 121 mg KYNA/ g LDH. This result is in good  
298 agreement with the experimentally determined value (~12%).

299

### 300 *3.2.1. PXRD analysis of KYNA intercalation*

301 Fig. 4 illustrates the PXRD patterns for the Mg/Al-LDH intercalated with KYNA compared  
302 with the initial LDH material. The intercalation of KYNA in LDH has significant influence on  
303 the PXRD pattern of LDH at pH=10. The well-crystallized LDH structure with a (003)  
304 diffraction peak positioned at an angle of  $11.39^\circ$  ( $2\Theta$ ) shows another (003) diffraction peak  
305 centered at 2.146 nm at a lower  $2\Theta$  angle ( $4.11^\circ$ ). The interlayer spacing increases by 1.371  
306 nm in comparison with initial positively charged LDH layers, which shows an interlayer  
307 spacing of 0.775 nm indicating the successful intercalation of drug anions between the  
308 interlayer regions.

309 As Cavani et al. (1991) mentioned, the thickness of the brucite-like layer of LDH is 0.48 nm,  
310 the gallery height in the KYNA-pillared material is 1.666 nm. A gallery height of 1.666 nm  
311 suggests a paraffin type monolayer arrangement (Betega de Paiva et al., 2008; Chiu et al.,  
312 2014) of the intercalated KYNA, with their main axis perpendicular to the layer and the anion  
313 carboxyl groups interacting with positively charged layer surfaces. The suspected structure,  
314 i.e. the paraffin type monolayer arrangement of the obtained LDH/ KYNA composite is also  
315 presented in Fig. 4.

316

### 317 *3.2.2. FT-IR spectra*

318 The FT-IR spectra of the KYNA intercalated in Mg/Al-LDH are presented in Fig. 5. The FT-  
319 IR spectra of initial LDH and pure KYNA are also illustrated for comparison. Fig. 5a shows  
320 the spectrum of nitrate-LDH, a broad absorption band at  $3450\text{ cm}^{-1}$  which is due to the  
321 stretching vibration of the hydroxyl groups of the LDH layers and water molecules from the



322 interlayer space. The band at  $1383\text{ cm}^{-1}$  was assigned to stretching vibration of  $\text{NO}_3^-$  (Aisawa  
323 et al., 2015). This strong absorption peak of the  $\text{NO}_3^-$  was decreased after the ion-exchanged  
324 reaction, supporting that  $\text{NO}_3^-$  was replaced by the KYNA molecule (Fig. 5b).  
325 In the spectrum of KYNA (Fig. 5c) the band at  $3474\text{ cm}^{-1}$  was derived from the stretching  
326 vibrations of  $-\text{O}-\text{H}$  bonds in the carboxyl group. The band centered at  $3431\text{ cm}^{-1}$  is due to  
327 OH bonded to the quinoline ring and the signal seen at  $3076\text{ cm}^{-1}$  is attributed to the C-H  
328 bonds of the quinoline ring. Furthermore, the band at  $2968\text{ cm}^{-1}$  corresponds to stretch  
329 vibrations of the C-H bonds of benzyl and quinoline rings and the signal at  $2718\text{ cm}^{-1}$   
330 corresponds to the double bond  $\text{N}=\text{C}$  in the quinoline ring (López et al., 2014). The  
331 asymmetric and symmetric COO stretching is obtained between  $1700\text{-}1400\text{ cm}^{-1}$ , those at  
332  $1631, 1595, 1415$  and  $1247\text{ cm}^{-1}$  were attributed to  $\nu(\text{C}=\text{O})$ ,  $\nu_{\text{as}}(\text{COO})$ ,  $\nu_{\text{s}}(\text{COO})$  and  $\nu(\text{C}-\text{N})$ ,  
333 respectively. (Geng et al., 2009; Ibrahim et al., 2005). After intercalation, the characteristic  
334 bands of KYNA were observed at  $1631, 1595, 1415, 1247\text{ cm}^{-1}$  in the case of KYNA/LDH  
335 (Fig. 5b). So, according to the evaluation of the IR spectra, the intercalation of KYNA  
336 molecules into the LDH lamellae was also proved.

337

### 338 3.2.3. Thermal analysis

339 Thermogravimetric analysis of the initial LDH clay and the synthesized composites provides  
340 useful information regarding the thermal stability and thermal decomposition temperature of  
341 the materials. The TG curve of powdered KYNA/ LDH pillared composite is illustrated in  
342 Fig. 6. The corresponding TG curves for pure KYNA and initial Mg/Al-LDH are also  
343 presented for comparison.

344 In the LDH, the thermal decomposition stages are generally overlapped and the exact  
345 temperature range of each stage depends largely on LDH type, heating rate and atmosphere  
346 ( $\text{N}_2$  or  $\text{O}_2$ ) (Benício et al., 2015). According to the literature data, LDH thermal behavior is

347 usually characterized by two main transition stages: (i) an endothermic process from room  
348 temperature to about 200 °C that corresponds to adsorbed and interlamellar water loss; this  
349 stage is reversible and occurs without lamellar structure collapse; and (ii) the second stage  
350 occurs with temperatures ranging from 200 to about 6-800 °C, and corresponds to lamellar  
351 hydroxyl group loss (dehydroxylation) as well as anions loss (Benício et al., 2015). In the case  
352 of our LDH sample, both weight losses can be observed. The interlamellar water content was  
353 15.7 wt.% (first step up until ~245 °C), while after about 650 °C, the remaining weight was  
354 53.7 wt.%. It can be also seen, that the heat degradation of the pure KYNA was occurred  
355 between 150 and 650 °C and after about this temperature, the mass loss of organic KYNA  
356 was complete (dashes line). Compared the corresponding TG curves, it can be determined that  
357 the remaining weigh difference between the KYNA/ LDH composite and the LDH sample  
358 was 13.9 wt.%. Fig. 3 shows that the maximum adsorption capacity of the LDH clay lamellae  
359 was about 120 mg KYNA/ g LDH. The thermogravimetric results were confirmed this ~12  
360 wt.% KYNA content of the KYNA pillared composite material.

361

### 362 3.3. Dissolution properties of LDH clay in SGF media

363 The dissolution properties of the LDH drug carrier in acidic pH was investigated  
364 gravimetrically and the acidic dissolution, i.e. the destruction of lamellae was also followed  
365 up by PXRD measurements (Fig. 7) The dissolution profile of LDH at pH= 1.5 was exhibited  
366 a very fast process: after about 30 minutes, more than 70 wt.% of the initial LDH weight was  
367 disappeared and at the end of the experiment, near 83% of LDH were completely dissolved in  
368 the applied SGF media after 360 minutes (Fig. 7a). The corresponding PXRD patterns of the  
369 LDH is presented in Fig. 7b and gives information about the LDH structure during the  
370 dissolution experiment. It can be observed that the intensity of the characteristic peaks of the  
371 well-crystallized LDH was continuously decreased, i.e. the (003) diffraction peak positioned

372 at an angle of  $11.39^\circ$  ( $2\Theta$ ) was shown decreasing intensity. This phenomenon is obviously  
373 due to dissolution of LDH drug carrier at pH= 1.5.

374

#### 375 3.4. *In vitro* drug release properties of the samples

376 The release properties of KYNA were studied at the pH of human saliva (Baliga et al., 2013;  
377 Pietrzyńska and Voelkel, 2017) at a value of 6.70 and at pH of SGF (pH=1.50), as well. The  
378 release study of the KYNA/LDH have also been performed at pH=1.5. Fig. 8 presents the  
379 drug release profiles which were carried out over a period of 240 min and at body temperature  
380 ( $37^\circ\text{C}$ ) and in physiological saline. The released concentration of drug were determined  
381 spectrophotometrically. The solubility and thus the release rate of anionic KYNA depends on  
382 pH (Varga et al., 2016). Thus, on Fig. 8a, a significant difference can be seen on the release  
383 rate of KYNA between pH= 6.70 and 1.50 under the same experimental condition. Due to the  
384 higher solubility of the KYNA molecules at pH= 6.70, the percentage amount of the released  
385 drug molecules were continuously increased up to 180 min and after three hours it was  
386 reached the 90% plateau value. However, at low pH (=1.50), the release of the KYNA was  
387 obviously slower process and the measured maximum value was only about 40%, because in  
388 this pH the KYNA molecules were formed heterogeneous precipitate instead of a clear  
389 homogenous solution (pH=6.70) (see inserted photos). In the case of KYNA release from  
390 concentrated solutions via the fitted (Fig. 8b) first-order rate model (Eq. 1) the following rate  
391 constant values ( $k$ ) were provided:  $4.74 \cdot 10^{-5} \text{ s}^{-1}$  and  $5.91 \cdot 10^{-5} \text{ s}^{-1}$  at pH=6.70 and pH=1.50,  
392 respectively. As regarding the composite sample, drug release profile for KYNA/LDH at pH=  
393 1.5 was exhibited a delayed drug release rate compared to the pure KYNA at the same pH.  
394 This is because the kinetic of the release process is controlled by the LDH, so the diffusion  
395 rate is significantly decreased. The determined  $k$  value was  $1.49 \cdot 10^{-5} \text{ s}^{-1}$  in this case. The  
396 corresponding half-life values ( $t_{1/2} = 4.1$  and  $3.3$  h for KYNA at pH=6.70 and 1.50,

397 respectively) are smaller than the half-life value of composite sample ( $t_{1/2} = 12.9$  h) at  
398 pH=1.50. The kinetic constant, release index and correlation coefficients ( $R^2$ ) values, which  
399 are summarised in Table 1 indicate what processes are controlled by the suggested release  
400 mechanism. Based on the values of correlation coefficients release of the KYNA from the  
401 KYNA/LDH composite was well described by the first-order rate model, while the drug  
402 release from concentrated solutions agreed with the Korsmeyer–Peppas model. The observed  
403 low release index values ( $n = 0.43$  and  $0.38$  for KYNA at pH=6.70 and 1.50, respectively)  
404 suggest the existing of Fickian diffusion mechanism which absolutely corresponds to the  
405 experimentally arranged conditions. Moreover, this model clearly shows the appearance of  
406 non Fickian diffusion ( $n = 0.46$  for KYNA/LDH at pH = 1.50) in the case of the composite  
407 where combination of drug diffusion and carrier erosion result the anomalous process.  
408 This result allows to conclude that the rate determining step for release of KYNA from the  
409 KYNA/LDH composite may be depending on the following conditions: (i) dissolution of  
410 LDH lamellae; (ii) ion-exchange reaction between KYNA and LDH and (iii) release of  
411 KYNA from LDH host lamellae. These data indicate that the Mg/Al-LDH could be an  
412 adequate drug carrier system for the neuroprotective and anti- ulcerant KYNA molecules at  
413 low pH.

414

#### 415 **4. Conclusions**

416 This study demonstrated the intercalation of anti- ulcerant KYNA molecules into a layered  
417 inorganic host, LDH, which was carried out with a simply ion- exchange reaction. The PXRD  
418 studies showed a paraffin type monolayer arrangement for anti-ulcerant drug molecules into  
419 the synthesized KYNA/ LDH hybrid material. The drug loading capacity of the 2:1 Mg/Al-  
420 LDH was studied by fluorescence spectroscopy method and the obtained ~12% KYNA  
421 content was in good agreement with the theoretical value calculated from the +0.641 meq/g

422 surface charge of the LDH lamellae. Moreover, this ~12% KYNA content of the hybrid  
423 materials was also confirmed by thermogravimetric (TG) measurements.  
424 Next, it was also demonstrated by gravimetric and PXRD measurements, that the prepared  
425 LDH was almost completely dissolved (~83 wt.%) in the applied simulated gastric fluid  
426 (SGF) media at pH=1.5. The *in vitro* release studies showed that due to the higher solubility  
427 of the KYNA molecules at pH= 6.70 a significant difference can be seen on the release rate of  
428 KYNA between pH= 6.70 ( $t_{1/2} = 4.1$  h) and 1.50 ( $t_{1/2} = 3.3$  h) under the same experimental  
429 condition. The drug release from KYNA/ LDH composite material at pH= 1.5 was observed a  
430 delayed drug release profile ( $1.49 \cdot 10^{-5} \text{ s}^{-1}$ ) compared to the pure KYNA ( $t_{1/2} = 12.9$  h) at the  
431 same pH. The obtained results gives a proof to us that the chosen LDH host molecule could  
432 be an adequate drug carrier system for the neuroprotective and anti- ulcerant KYNA  
433 molecules at gastric pH, used for peptic ulcer diseases.

434

#### 435 **Acknowledgements**

436 The authors are very thankful for the financial support from the Hungarian Scientific  
437 Research Fund (OTKA) K 116323 and the project named GINOP-2.3.2-15-2016-00034. This  
438 paper was supported by the János Bolyai Research Scholarship of the Hungarian Academy of  
439 Sciences (E. Csapó). This paper was supported by the UNKP-17-4 New National Excellence  
440 Program of the Ministry of Human Capacities (L. Janovák).

441

#### 442 **References**

443 Aisawa, S., Ohnuma, Y., Hirose, K., Takahashi, S., Hirahara, H., Narita, E., 2015.  
444 Intercalation of nucleotides into layered double hydroxides by ion-exchange reaction. Applied  
445 Clay Science. 28, 137– 145.

446 Baliga, S., Muglikar, S., Kale, R., 2013. Salivary pH: A diagnostic biomarker. *J. Indian Soc.*  
447 *Periodontol.* 17 (4), 461–465.

448 Benício, L. P. F., Silva, R. A., Lopes, J. A., Eulálio, D., Menezes dos Santos, R. M., Angelo  
449 de Aquino, L., Vergütz, L., Novais, R. F., Marciano da Costa, L., Pinto, F. G., Tronto, J.,  
450 2015. Layered double hydroxides: nanomaterials for applications in agriculture, *R. Bras. Ci.*  
451 *Solo.* 39, 1-13.

452 Betega de Paiva, L., Morales, A. R., Valenzuela Díaz, F.R., 2008. Organoclays: Properties,  
453 preparation and applications. *Applied Clay Science.* 42, 8–24.

454 Bish, D.L., 1980. Anion exchange in takovite: application to other hydroxide minerals. *Bull.*  
455 *Mineral.* 103, 170–175.

456 Bujdosó, T., Patzkó, Á., Galbács, Z., Dékány, I., 2009. Structural characterization of arsenate  
457 ion exchanged MgAl-layered double hydroxide. *Applied Clay Science* 44, 75–82.

458 Cavani, F., Trifiro, F., Vaccari, A., 1991. Hydrotalcite-type anionic clays: preparation,  
459 properties and applications. *Catal. Today* 11, 173–301.

460 Chiu, C.-W., Huang, T.-K., Wang, Y.-C., Alamani, B. G., Lin, J.-J., 2014. Intercalation  
461 strategies in clay/polymer hybrids. *Progress in Polymer Science.* 39, 443–48.

462 Choy J.-H., Jung, J.-S., Oh, J.-M., Park, M., Jeong, J., Kang, Y.-K., Han, O.-J. 2004. Layered  
463 double hydroxide as an efficient drugreservoir for folate derivatives. *Biomaterials* 25, 3059-  
464 3064.

465 Choy, J.-H., Choi, S.-J., Oh, J.-M., Park, T., 2007. Clay minerals and layered double  
466 hydroxides for novel biological applications. *Applied Clay Science.* 36, 122–132.

467 Constantino, U., Nocchetti, M., 2001. Layered Double Hydroxides and Their Intercalation  
468 Compounds in Photochemistry and Medicinal Chemistry. In: Rives, V. (Ed); *Layered Double*  
469 *Hydroxides: Present and Future*, Nova Science Publishers: New York, pp. 383–412.

470 Costa, F. R., Leuteritz, A., Wagenknecht, U., Jehnichen, D., Häußler, L., Heinrich, G., 2008.  
471 Intercalation of Mg–Al layered double hydroxide by anionic surfactants: Preparation and  
472 characterization. *Applied Clay Science*. 38, 153–164.

473 Costa, P., Lobo, J. M. S., 2001. Modeling and comparison of dissolution profiles. *European*  
474 *Journal of Pharmaceutical Sciences* 13, 123–133.

475 Cunha, A. S., Grossiord, J. L., Puisieux, F., Seiller, M., 1997. Insulin in w/o/w multiple  
476 emulsions: preparation, characterization and determination of stability towards proteases in  
477 vitro. *J. Microencapsul.* 14, 311–319.

478 Cunha, V. R. R., Barbosa de Souza, R., Rebello Pinto da Fonseca Martins, A. M. C., Koh, I.  
479 H. J., Leopoldo Constantino, V. R., 2016. Accessing the biocompatibility of layered double  
480 hydroxide by intramuscular implantation: histological and microcirculation evaluation. *Nature*  
481 *Scientific reports*. DOI: 10.1038/srep30547.

482 Deák, Á., Janovák, L., Tallósy, Sz. P., Bitó, T., Sebők, D., Buzás, N., Pálinkó, I., Dékány, I.,  
483 2015. Spherical LDH–Ag<sup>0</sup>-Montmorillonite Heterocoagulated System with a pH-Dependent  
484 Sol–Gel Structure for Controlled Accessibility of AgNPs Immobilized on the Clay Lamellae.  
485 *Langmuir*. 31, 2019–2027.

486 Deák, Á., Janovák, L., Csapó, E., Ungor, D., Pálinkó, I., Puskás, S., Ördög, T., Ricza, T.,  
487 Dékány, I., 2016. Layered double oxide (LDO) particle containing photoreactive hybrid layers  
488 with tunable superhydrophobic and photocatalytic properties. *Applied Surface Science* 389,  
489 294–302.

490 Deng, L., Shi, Z., Xiaoxu Peng, X. 2015. Adsorption of Cr(VI) onto a magnetic CoFe<sub>2</sub>O<sub>4</sub>/  
491 MgAl-LDH composite and mechanism study. *RSC Adv.*, 5, 49791–49801.

492 Frenning, G., 2011. Modelling drug release from inert matrix systems: From moving-  
493 boundary to continuous-field descriptions. *International Journal of Pharmaceutics* 418, 88–99.

494 Fudala, Á., Pálinkó, I., Kiricsi, I., 1999. Amino acids, precursors for cationic and anionic  
495 intercalation synthesis and characterization of amino acid pillared materials. *J. Mol. Struct.*  
496 482-483, 33–37.

497 Geng, W., Nakajima, T., Takanashi, H., Akira Ohki, A., 2009. Analysis of carboxyl group in  
498 coal and coal aromaticity by Fourier transform infrared (FT-IR) spectrometry. *Fuel.* 88, 139–  
499 144.

500 Glavin, G. B., Bose, R., Pinsky, C., 1989. Kynurenic acid protects against gastroduodenal  
501 ulceration in mice injected with extracts from poisonous atlantic shellfish. *Prog. Neuro-*  
502 *Psychopharmacol.* 6 *Biol. Psychiat.* 13, 569-572.

503 Glavin, G. B., Pinsky, C., 1989. Kynurenic acid attenuates experimental ulcer formation and  
504 basal gastric acid secretion in rats. *Res Commun Chem Pathol Pharmacol.* 64 (1), 111-119.

505 Goh, K.-H., Lim, T.-T., Dong, Z.L., 2008. Application of layered double hydroxides for  
506 removal of oxyanions: A review. *Water Res.* 42, 1343–1368.

507 Guérin, D., Vuilleumard, J.-C., Subirade, M., 2003. Protection of Bifidobacteria Encapsulated  
508 in Polysaccharide-Protein Gel Beads against Gastric Juice and Bile. *Journal of Food*  
509 *Protection,* 66 (11), 2076–2084

510 Ibrahim, M., Nada, A., Kamal, D. E., 2005. Density functional theory and FTIR spectroscopic  
511 study of carboxyl group. *Indian Journal of Pure & Applied Physics.* 43, 911-917.

512 Joshi, G. V., Patel, H. A., Bajaj, H. C., Jasra, R. V. 2009. Intercalation and controlled release  
513 of vitamin B6 from montmorillonite–vitamin B6 hybrid. *Colloid Polym Sci* 287, 1071–1076.

514 Juhász, Á., Csapó, E., Ungor, D., Tóth, G. K., Vécsei, L., Dékány, I., 2016. Kinetic and  
515 Thermodynamic Evaluation of Kynurenic Acid Binding to GluR1270–300 Polypeptide by  
516 Surface Plasmon Resonance Experiments. *J. Phys. Chem. B.* 120, 7844–7850.

517 Kevadiya, B. D., Joshi, G. V., Patel, H. A., Ingole, P. G., Mody, H. M., Bajaj, H. C. 2010.  
518 Montmorillonite-Alginate Nanocomposites as a Drug Delivery System: Intercalation and In



519 Vitro Release of Vitamin B<sub>1</sub> and Vitamin B<sub>6</sub>. *Journal of biomaterials applications* 25 (2), 161-  
520 177.

521 Li, B., He, J., Evans, D.G., Duan, X., 2004. Inorganic layered double hydroxides as a drug  
522 delivery system-intercalation and in vitro release of fenbufen. *Appl. Clay Sci.* 27, 199–207.

523 López, T., Ortiz, E., Gómez, E., Pérez-de la Cruz, V., Carrillo-Mora, P., Novaro, O., 2014.  
524 Preparation and Characterization of Kynurenic Acid Occluded in Sol-Gel Silica and SBA-15  
525 Silica as Release Reservoirs. *Journal of Nanomaterials*. 2014, 8.

526 Marosi, M., Nagy, D., Farkas, T., Kis, Z., Rózsa, É., Robotka, H., Fülöp, F., Vécsei, L., Toldi,  
527 J., 2010. A novel kynurenic acid analogue: a comparison with kynurenic acid, An in vitro  
528 electrophysiological study. *J. Neural. Transm.* 117, 183–188.

529 Nagy, K., Bíró, G., Berkesi, O., Benczédi, D., Ouali, L., Dékány, I., 2013. Intercalation of  
530 lecithins for preparation of layered nanohybrid materials and adsorption of limonene. *Applied*  
531 *Clay Science*. 72, 155–162.

532 Oh, J.-M., Choi, S.-J., Kim, S.-T., Choy, J.-H., 2006. Cellular uptake mechanism of an  
533 inorganic nanovehicle and its drug conjugates: Enhanced efficacy due to clathrin-mediated  
534 endocytosis. *Bioconjug. Chem.* 17, 1411–1417.

535 Oh, M.-J., Biswick, T. T., Choy, J.-H., 2009. Layered nanomaterials for green materials. *J.*  
536 *Mater. Chem.* 19, 2553–2563.

537 Patzkó, Á., Kun, R., Hornok, V., Dékány, I., Engelhardt, T., Schall, N., 2005. ZnAl-layer  
538 double hydroxides as photocatalysts for oxidation of phenol in aqueous solution. *Colloids and*  
539 *Surfaces A: Physicochem. Eng. Aspects* 265, 64–72.

540 Peppas, N. A., Merrill, E. W., 1977. Crosslinked Poly( vinyl Alcohol) Hydrogels as Swollen  
541 Elastic Networks, *Journal of Applied Polymer Science* 21, 1763-1770.

542 Patel, H. A., Shah, S., Shah, D. O., Joshi, P. A. 2011. Sustained release of venlafaxine from  
543 venlafaxine–montmorillonite–polyvinylpyrrolidone composites. *Applied Clay Science* 51,  
544 126–130.

545 Pietrzyńska, M., Voelkel, A., 2017. Stability of simulated body fluids such as blood plasma,  
546 artificial urine and artificial saliva. *Microchemical Journal*. 134, 197–201.

547 Posati, T., Bellezza, F., Tarpani, L., Perni, S., Latterini, L., Marsili, V., Cipiciani, A., 2012.  
548 Selective internalization of ZnAl–HTlc nanoparticles in normal and tumor cells. A study of  
549 their potential use in cellular delivery. *Appl. Clay Sci.* 55, 62–69.

550 Siepmann, J., Peppas, N. A., 2011. Higuchi equation: Derivation, applications, use and  
551 misuse, *International Journal of Pharmaceutics* 418, 6–12.

552 Szabó, T., Veres, Á., Cho, E., Khim, J., Varga, N., Dékány, I., 2013. Photocatalyst separation  
553 from aqueous dispersion using graphene oxide/TiO<sub>2</sub> nanocomposites. *Coll. Surf. A.* 433,  
554 230–239.

555 Tarnawski, A.S., Tomikawa, M., Ohta, M., Sarfeh, I.J., 2000. Antacid talcid activates in  
556 gastric mucosa genes encoding for EGF and its receptor. The molecular basis for its ulcer  
557 healing action. *J. Physiol., Paris* 94, 93–98.

558 Trifiro, F., Vaccari, A., 1996. Hydrotalcite-like anionic clays (layered double hydroxides).  
559 *Compr. Supramol. Chem.* 7, 251–291.

560 Turski, M. P., Turska, M., Paluszkiewicz, P., Parada-Turska, J., Oxenkrug, G. F., 2013.  
561 Kynurenic Acid in the Digestive System—New Facts, New Challenge. *International Journal*  
562 *of Tryptophan Research.* 6, 47–55.

563 Varga, N., Csapó, E., Majláth, Z., Ilisz, I., Krizbai, I. A., Wilhelm, I., Knappe, L., J. Toldi, J.,  
564 Vécsei, L., Dékány I., 2016. Targeting of the kynurenic acid across the blood–brain barrier by  
565 core-shell nanoparticles. *European Journal of Pharmaceutical Sciences* 86, 67–74.

566 Yang, J.H., Lee, S.Y., Han, Y.S., Park, K.C., Choy, J.H., 2003. Efficient transdermal  
567 penetration and improved stability of L-ascorbic acid encapsulated in an inorganic  
568 nanocapsule. Bull. Korean Chem. Soc. 24, 499–503.

569

570 **Figure 1.** PXRD pattern of the synthesized 2:1 Mg/Al LDH powder (a) and the charge  
571 titration curve of 0.1 wt.% cationic LDH suspension (pH=10) with 0.1 wt.% of anionic  
572 sodium dodecyl sulfate (NaDS) surfactant solution (b).

573 **Figure 2.** Adsorption isotherms of N<sub>2</sub> at 77 K on LDH powder sample (a). The inserted figure  
574 shows the corresponding deBoer *t*-plot of the same sample (b).

575 **Figure 3.** The effect of the KYNA weight ratio on the intercalation capacity of the KYNA  
576 molecules loaded LDH layers

577 **Figure 4.** PXRD patterns of the initial LDH lamellae and KYNA molecules intercalated into  
578 the LDH layers and the proposed structure of KYNA-LDH composite

579 **Figure 5.** FT-IR spectra for (a) LDH drug carrier, (b) KYNA-LDH composite and (c) KYNA  
580 powder samples

581 **Figure 6.** TG profiles for LDH drug carrier, KYNA-LDH composite and initial KYNA

582 **Figure 7.** The gravimetrically measured percentage weight loss of the LDH drug carrier in  
583 SGF media at pH= 1.5 (a) and the corresponding PXRD patterns of LDH sample during the  
584 dissolution process (b).

585 **Figure 8.** The percentage release profile of anionic KYNA molecules at two different pH  
586 values (pH= 6.70 and 1.50) and the KYNA release from LDH lamellae at acidic (pH= 1.50)  
587 pH, as well as the measured KYNA concentration values (C<sub>t</sub>, mg/ mL) as a function of release  
588 time with the fitted curves calculated by the first-order rate model

589 **Table 1.** Interpretation of the release experiments using different various models.

## Anti-ulcerant kynurenic acid molecules intercalated Mg/Al-layered double hydroxide and its release study

Ágota Deák<sup>a</sup>, Edit Csapó<sup>a,b</sup>, Ádám Juhász<sup>a,b</sup>, Imre Dékány<sup>a,b</sup>, László Janovák<sup>a,\*</sup>

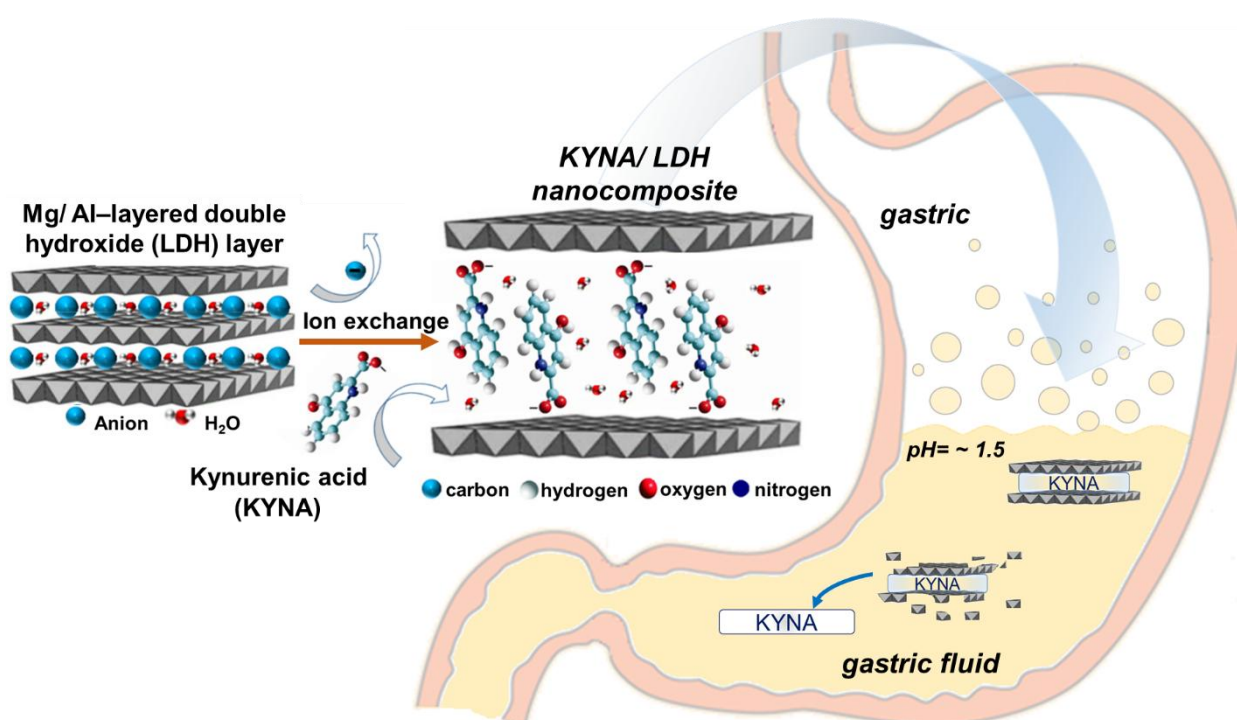
<sup>a</sup>Department of Physical Chemistry and Materials Science, University of Szeged, H-6720, Szeged, Rerrich B. tér 1, Hungary

<sup>b</sup>MTA-SZTE Biomimetic Systems Research Group, University of Szeged, H-6720, Szeged, Dóm tér 8, Hungary

\* Corresponding authors. Tel.: +36 62 544 210; Fax: +36 62 544 042.

E-mail address: [janovakl@chem.u-szeged.hu](mailto:janovakl@chem.u-szeged.hu) (L. Janovák)

### Graphical abstract



## Highlights

- LDH was synthesized as inorganic drug carrier system for kynurenic acid molecules
- KYNA molecules exhibited paraffin type monolayer arrangement in LDH lamellae
- LDH layers were almost completely dissolved at gastric pH during the *in vitro* study
- The anti-ulcerant KYNA molecules were released from the destroyed interlayers

**Table 1**

Kinetic models	<i>KYNA pH= 6.70</i>		<i>KYNA pH= 1.50</i>		<i>KYNA/LDH pH= 1.50</i>	
	37°C		37°C		37°C	
	<i>k</i>	<i>R</i> <sup>2</sup>	<i>k</i>	<i>R</i> <sup>2</sup>	<i>k</i>	<i>R</i> <sup>2</sup>
First order Model (s <sup>-1</sup> )	4.75 x 10 <sup>-5</sup>	0.9955	5.91 x 10 <sup>-5</sup>	0.8363	1.49 x 10 <sup>-5</sup>	0.9045
Korsmeyer–Peppas Model (s <sup>-n</sup> )	1.62 x 10 <sup>0</sup>	0.9524	1.26 x 10 <sup>0</sup>	0.9506	1.90 x 10 <sup>-1</sup>	0.8361
Higuchi Model (s <sup>-1/2</sup> )	8.88 x 10 <sup>-3</sup>	0.9389	8.51 x 10 <sup>-1</sup>	0.9261	8.57 x 10 <sup>-1</sup>	0.8467

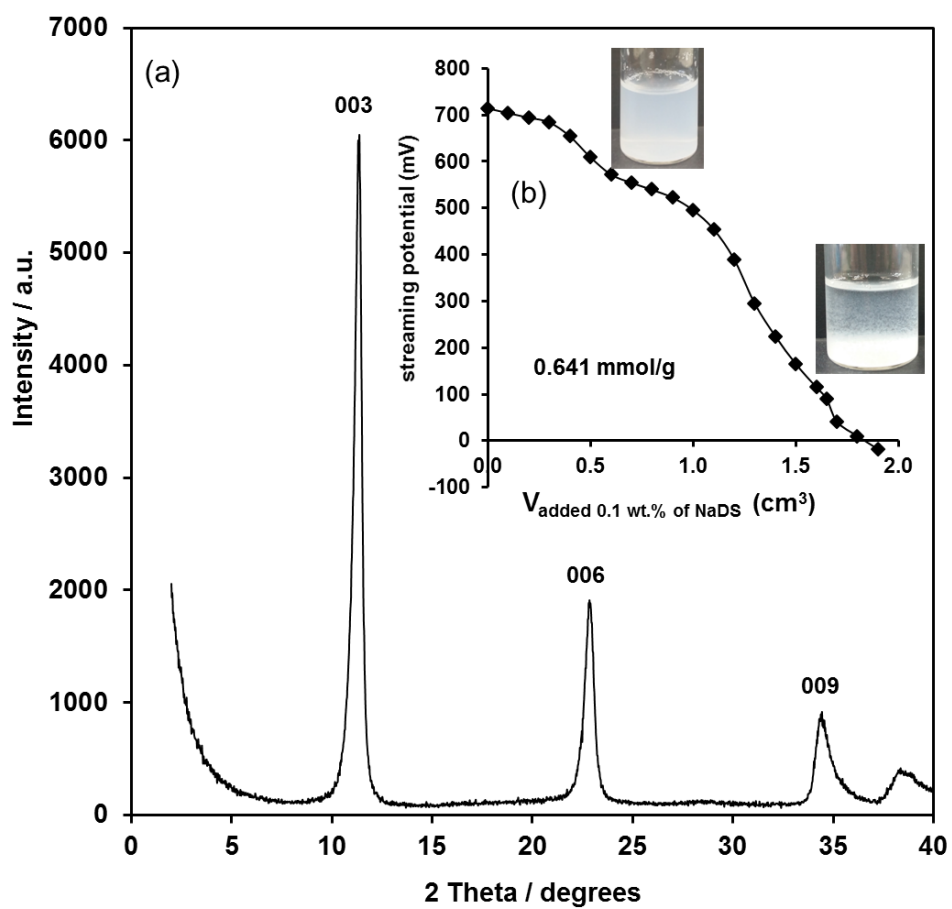


Figure 1.



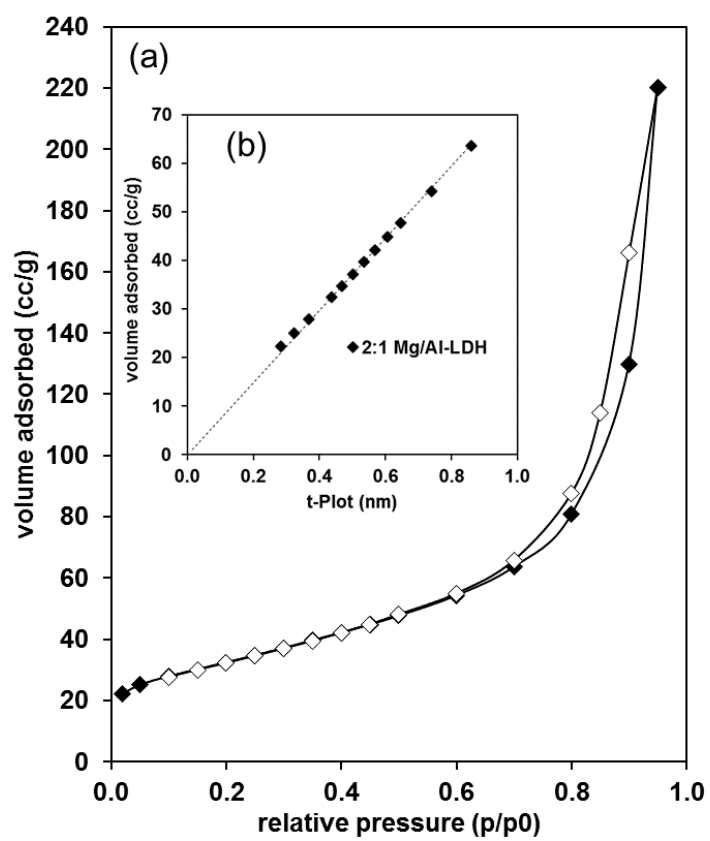
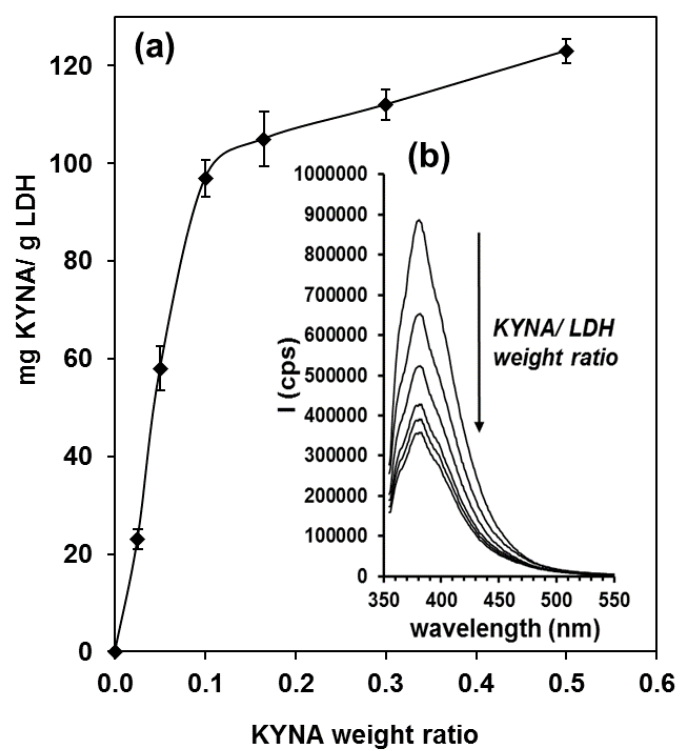


Figure 2.



**Figure 3.**

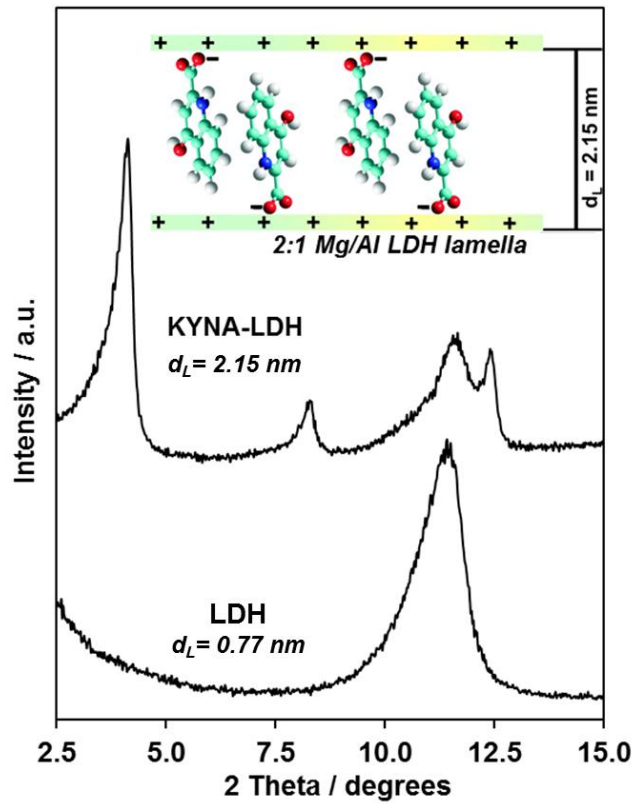


Figure 4.

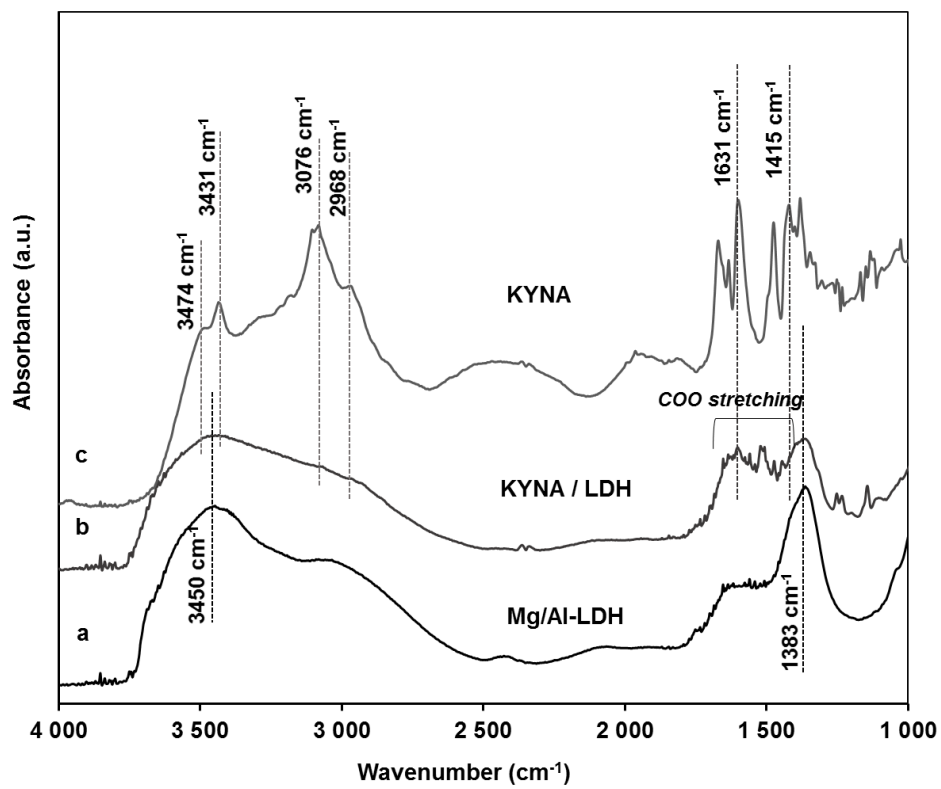
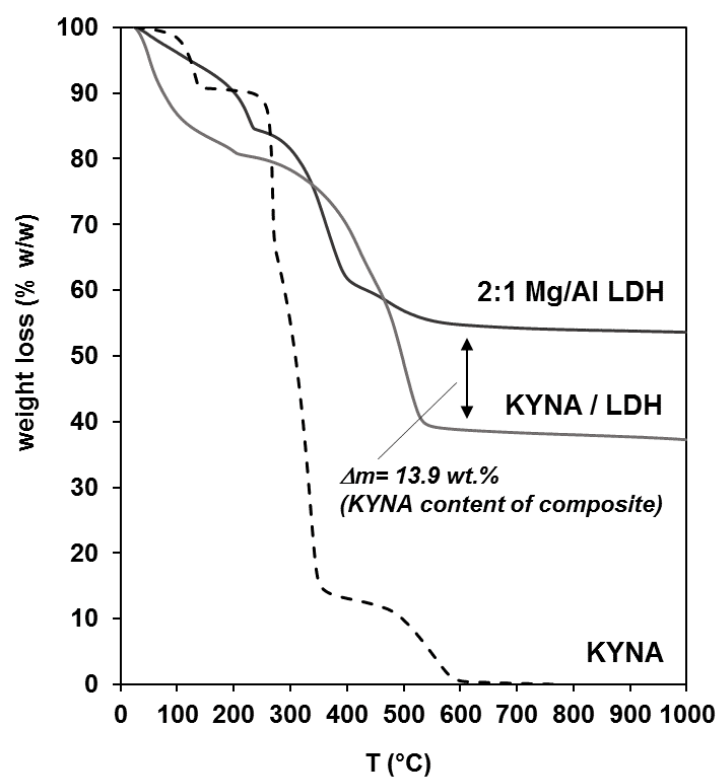
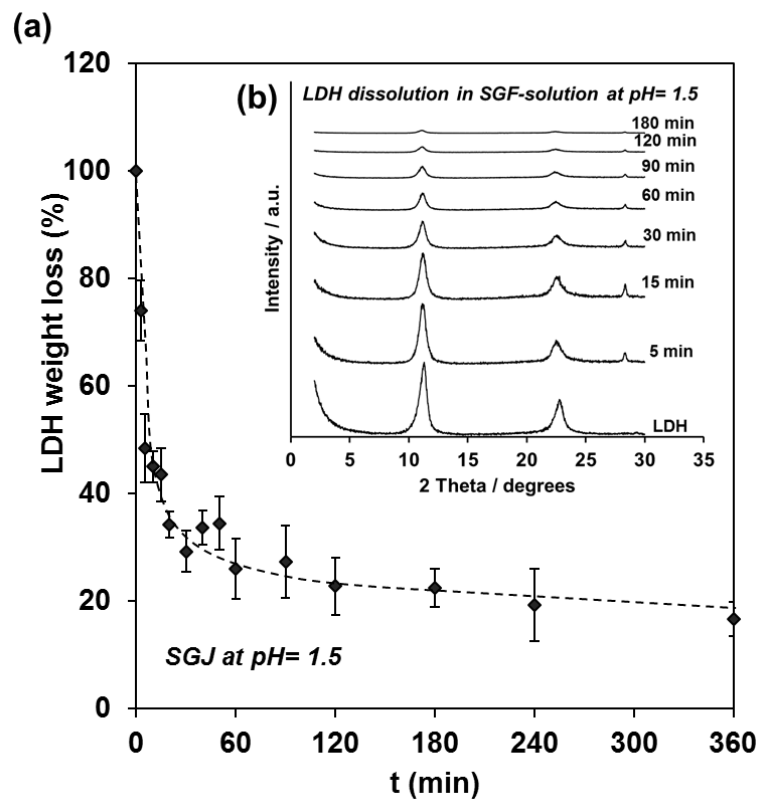


Figure 5.



**Figure 6.**



**Figure 7.**

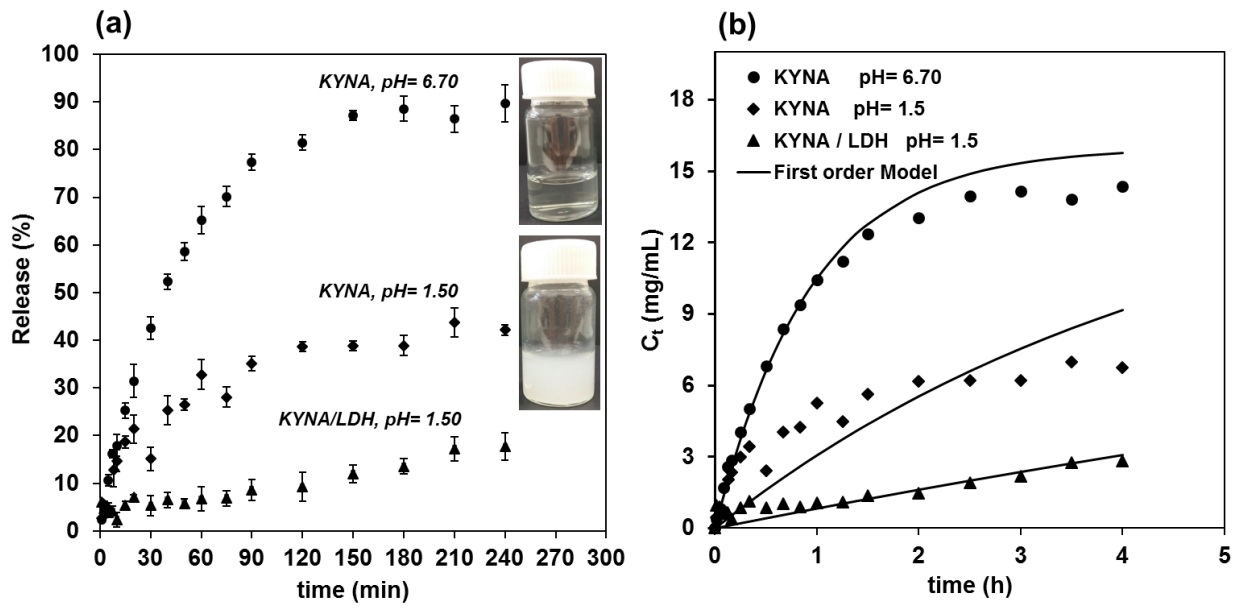


Figure 8.

1     **Anti-ulcerant kynurenic acid molecules intercalated Mg/Al-layered double hydroxide**  
2   **and its release study**

3

4             Ágota Deák<sup>a</sup>, Edit Csapó<sup>a,b</sup>, Ádám Juhász<sup>a,b</sup>, Imre Dékány<sup>a,b</sup>, László Janovák<sup>a,\*</sup>

5     <sup>a</sup>*Department of Physical Chemistry and Materials Science, University of Szeged, H-6720,*  
6     *Szeged, Rerrich B. tér 1, Hungary*

7     <sup>b</sup>*MTA-SZTE Biomimetic Systems Research Group, University of Szeged, H-6720, Szeged,*  
8     *Dóm tér 8, Hungary*

9

10     \* Corresponding authors. Tel.: +36 62 544 210; Fax: +36 62 544 042.

11     *E-mail address: [janovakl@chem.u-szeged.hu](mailto:janovakl@chem.u-szeged.hu) (L. Janovák)*

12

13

14     **Abstract**

15     Kynurenic acid (KYNA) is a product of the tryptophan metabolism and it possess also anti-  
16     ulcerant properties, however, the application of KYNA for the treatment of gastroduodenal  
17     ulceration is limited, because the concentration of KYNA is very low in human gastric fluid  
18     (0.01  $\mu\text{M}$ ). The intercalation of KYNA molecules into biocompatible Mg–Al layered double  
19     hydroxides (LDH) lamellae could solve this problem. For this purpose Mg–Al LDH with  
20      $114.96 \pm 0.48 \text{ m}^2/\text{g}$  BET surface area and  $+0.641 \text{ meq/g}$  specific surface charge was  
21     synthesized. The intercalation of the anionic target molecules into positively charged LDH  
22     layers was carried out with simply ion- exchange reaction. The structure of the obtained  
23     KYNA/ LDH hybrid materials were studied by powdered X-ray diffraction (PXRD) and  
24     Attenuated total reflection Fourier transform infrared (ATR-FTIR) spectroscopy verifying that  
25     the KYNA molecules prefer creating a paraffin type monolayer arrangement. Due to the



26 intercalation process the (003) reflection peaks of initial LDH ( $2\Theta= 11.39^\circ$ ,  $d_{(003)}= 0.775$  nm)  
27 shift to lower angles ( $2\Theta= 4.11^\circ$ ,  $d= 2.146$  nm). That means, that the basal space value ( $\Delta d_L$ )  
28 of the KYNA-LDH sample was 1.436 nm. The total amount of the intercalated KYNA  
29 molecules into LDH layers was measured by fluorescence spectroscopy method. According to  
30 the results the drug- loading capacity was about 120 mg KYNA/ g LDH. This ~12% KYNA  
31 content of the hybrid materials was also evidenced by thermogravimetric measurements,  
32 because the thermal decomposition of the bio-hybrid materials was examined by  
33 thermogravimetry (TG) analysis. Our experimental data confirm that the anti- ulcerant KYNA  
34 molecules can be safely loaded and stored into LDH's layers forming a new bio-active hybrid  
35 material. In addition we also presented by PXRD and gravimetric measurements that prepared  
36 LDH layers were almost completely dissolved (~83 wt.%) in the applied simulated gastric  
37 fluid (SGF) media (pH=1.5) under 60 min and the encapsulated KYNA molecules released  
38 from the destroyed interlayers. Finally, the measured KYNA drug release profile from the  
39 bioactive composite material was also presented in SGF media. According to the results 18%  
40 of the loaded KYNA molecules were released during 6 hours.

41

42 **Keywords:** layered double hydroxide, kynurenic acid, intercalation, *in vitro* drug release  
43 study, anti- ulcerant properties, simulated gastric fluid